

# Satellite lines from autoionizing states of Fe XVI and the problems with the X-ray Fe XVII lines

G. Del Zanna<sup>1\*</sup>, N. R. Badnell<sup>2</sup>, P. J. Storey<sup>3</sup>

<sup>1</sup> DAMTP, Centre for Mathematical Sciences, University of Cambridge, Wilberforce Road, Cambridge CB3 0WA, UK

<sup>2</sup> Department of Physics, University of Strathclyde, Glasgow, G4 0NG, UK

<sup>3</sup> Department of Physics and Astronomy, University College London, London WC1E 6BT, UK

Submitted to MNRAS

## ABSTRACT

We present new calculations of atomic data needed to model autoionizing states of Fe xvi. We compare the state energies, radiative and excitation data with a sample of results from previous literature. We find a large scatter of results, the most significant ones in the autoionization rates, which are very sensitive to the configuration interaction and state mixing. We find relatively good agreement between the autoionization rates and the collisional excitation rates calculated with the *R*-matrix suite of programs and *AUTOSTRUCTURE*. The largest model, which includes *J*-resolved states up to  $n = 10$ , produces ab-initio wavelengths and intensities of the satellite lines which agree well with solar high-resolution spectra of active regions, with few minor wavelength adjustments. We review previous literature, finding many incorrect identifications, most notably those in the NIST database. We provide several new tentative identifications in the 15–15.7 Å range, and several new ones at shorter wavelengths, where previous lines were unidentified. Compared to the previous CHIANTI model, the present one has an increased flux in the 15–15.7 Å range at 2 MK of a factor of 1.9, resolving the discrepancies found in the analysis of the Marshall Grazing Incidence X-Ray Spectrometer (MaGIXS) observation. It appears that the satellite lines also resolve the long-standing discrepancy in the intensity of the important Fe xvii 3D line at 15.26 Å.

**Key words:** atomic data – atomic processes – Sun: X-rays

## 1 INTRODUCTION

The Marshall Grazing Incidence X-Ray Spectrometer (MaGIXS) flew in 2021 on a sounding rocket and produced the first ever spectral-imaging data of the solar corona in the X-rays, between about 6 and 30 Å (Savage et al. 2023). The instrument had a wide slit and produced spectroheliograms of an X-ray bright point, which had a temperature of about 2 MK. The strongest emission lines in the spectra were from O vii, O viii, and the Fe xvii lines between 15 and 17 Å. As discussed by Savage et al. (2023), the modelling of the spectra with the CHIANTI<sup>1</sup> version 10 atomic data (Del Zanna et al. 2021) was satisfactory, except the region between 15 and 15.6 Å, where the predicted model was lower by nearly a factor of 2. This is the important spectral region where the strong Fe xvii resonance and intercombination lines (3C at 15.0 and 3D at 15.26 Å) are present.

Possible calibration problems were excluded, which pointed to a problem in the atomic data. Such a large discrepancy was at first surprising, as *R*-matrix scattering calculations (cf

Hummer et al. 1993; Berrington et al. 1995) such as those of Loch et al. (2006); Liang & Badnell (2010) resolved the main long-standing discrepancies between predicted and observed intensities of the strongest Fe xvii lines. Indeed, Del Zanna (2011) showed excellent agreement, to within 10%, between line intensities calculated with those *R*-matrix rates and a sample of solar high-resolution observations of active regions and flares. However, two of the weaker lines, the 3D at 15.26 Å and the line at 15.45 Å were shown by Del Zanna (2011) to be significantly blended in quiescent active region observations, where the plasma has a temperature of about 3 MK.

The discrepancies between theory and observation of the Fe xvii lines, and in particular that of the 3C/3D lines has been the subject of well over 100 publications, many of which are referenced by Kühn et al. (2022). Such interest in the literature is because Fe xvii provides the strongest lines in the X-rays in laboratory and astrophysical spectra. It is also worth noting that the strong Fe xvii lines can be used to measure the electron temperature, as confirmed for the first time in Del Zanna (2011) [this diagnostic was previously known but the earlier atomic data did not allow such a diagnostic to be used].

It has been known for a long time that satellite lines of Ne-like

\* E-mail: gd232@cam.ac.uk

<sup>1</sup> www.chiantidatabase.org

iron (Fe xvii), i.e. decays to bound states from autoionizing (AI) states of Na-like Fe xvi are present in the 14–18 Å range and blend several Fe xvii lines, although a clear picture of their intensities and wavelengths has not emerged from previous literature, as described below. These satellite lines are expected to be much stronger (relative to Fe xvii) in low-temperature 2 MK plasma. Therefore, they are the likely candidates for the missing flux in the MaGIXS spectra, also considering that the CHIANTI model for these lines was limited.

We present in this paper a selection of results from several new atomic calculations we have carried out and used to calculate the intensities of these satellite lines. The main aim of the paper is to show that indeed the missing flux in the MaGIXS spectra is mainly due to satellite lines from AI states of Na-like Fe xvi. We also note that satellite lines from AI states of Fe xv have also been observed in the same spectral region. We have carried out a preliminary calculation for the satellites from Fe xv but found them much weaker than the Fe xvi lines. The present and further studies are part of a long-term programme within the UK APAP network<sup>2</sup> to provide accurate atomic data for astrophysics and laboratory plasma.

The presence of the Fe xvi satellite lines needs to be carefully taken into account when dealing with the Fe xvii lines for their diagnostic use. Another reason why this work is important is that the satellite lines, once their identification and atomic data are firmly established, could be used for a wide range of unique diagnostic applications for solar active regions but also in general for astrophysical plasma. These include measuring electron temperatures, departures from ionization equilibrium or non-Maxwellian electron distributions. Satellite lines are usually formed by both inner-shell (IS) excitation and dielectronic capture (DC). Seminal papers are Gabriel & Paget (1972); Gabriel (1972), while useful reviews are those of Dubau & Volonte (1980); Del Zanna & Mason (2018). As described in these reviews, insofar as the various diagnostics have only been applied to satellites of He-like ions, hence to very high temperature plasma as in solar flares. Therefore, the Fe xvi satellite lines offer in principle new diagnostic tools to study much lower temperature plasmas, typical of solar active regions.

Section 2 gives a summary of relevant previous studies. Section 3 describes the methods and presents a sample of results with some comparisons with previous calculations. Section 4 gives a sample of comparisons with solar data, while Section 5 gives the conclusions. A full set of atomic data in CHIANTI format is provided online via ZENODO.

## 2 EARLIER STUDIES

We now give a brief summary of the main studies on Fe xvi autoionizing states which are relevant to the present work, in chronological order. Unfortunately, none of the studies we have found in the literature provided a complete set of data (even radiative) that we could use to build a model for comparison with ours. We have also tried to carry out in-depth comparisons with the results in the literature, but very often it has been impossible to identify states. This is not because of the different coupling schemes, but because the very strong mixing within almost all the AI states means that only the energy, parity and  $J$  could be used to try and identify states and transitions. The  $L$ ,  $S$  quantum numbers and even the configuration are often not useful. As some AI states with the same parity and  $J$  are very close

in energy, the ordering and mixing of states changes considerably from calculation to calculation. It is therefore impossible to even attempt firm comparisons with other calculations when the full set of states is not provided.

Burkhalter et al. (1979) presented laser spectra in the 15.4–16.4 and 16.8–18.0 Å ranges. The spectra had a good resolution, as they were obtained with a 3-m grazing incidence spectrometer. The spectra contained the satellite lines from Fe xvi but also satellite lines from Fe xv and many strong Fe xvii, Fe xviii transitions. Cowan’s multi-configurational Hartree-Fock code was used to attempt the identification of several Fe xvi lines from  $n = 3$  states. It was clear that satellite lines are blended with many of the strong Fe xvii lines. There were significant discrepancies between the predicted (relative) intensities and the observed ones, as well as between the predicted and observed wavelengths. As the authors pointed out, the identifications were very difficult, partly because all the lines were blended, partly because the procedure was not aided by studies along the sequence (they also analysed similar spectra from Ti). Despite this, several experimental energies appeared in the NIST database (Kramida et al. 2022) from a reanalysis of the Burkhalter et al. (1979) observations. Details can be found e.g. in Shirai et al. (2000). The NIST experimental energies were included in the CHIANTI v.9 (Dere et al. 2019) model. As we shall see below, several of the NIST experimental energies are clearly incorrect. Inconsistencies in the Burkhalter et al. (1979) identifications were found, although the information was not sufficient to produce a full assessment.

Jupen et al. (1988) revised a previous identification of a single decay among the AI states, observed with the beam-foil method: the  $2p^5 3s3p \ ^4D_{7/2} - 2p^5 3s3d \ ^4F_{9/2}$  transition was identified with a line they observed at  $248.36 \pm 0.05$  Å.

Cornille et al. (1994) provided a limited set of atomic data for the  $n = 3$  satellite lines, calculated with the SUPERSTRUCTURE code. Only the total intensity factor  $F_2$  (see below) was provided, along with predicted wavelengths, and a few cross-sections for inner-shell excitation. Some general comparisons with SMM/FCS spectra were provided.

Phillips et al. (1997) used Cowan’s code to calculate intensities of the  $n = 3, 4, 5$  satellite lines. Although the paper was focused on the Fe xvii lines, the authors provided a table of the strongest  $n = 3$  lines formed by DC, also providing a comparison with the Cornille et al. (1994) results. Unfortunately, only a few transitions were listed, and only the total intensity factor  $F_2$  was provided, along with predicted wavelengths. We do attempt to match the states, and provide a comparison with our data below. Some general comparisons with SMM/FCS spectra were also provided.

Bruch et al. (1998) presented radiative data for the  $n = 3, 4$  states calculated with Cowan’s code and compared them to those calculated earlier by Nilsen (1989) with YODA, a relativistic multi-configurational Dirac-Fock code. We refer to their tables below when we compare our data with theirs. Unfortunately, the authors only published (total) weighted radiative rates and AI rates.

Brown et al. (2001) provided laboratory evidence that at least three IS satellite lines are present, at 15.12, 15.21, and 15.26 Å. The latter is blending the strong Fe xvii intercombination 3D line. They presented low-resolution X-ray spectra obtained with the Lawrence Livermore National Laboratory (LLNL) electron beam ion trap (EBIT).

Safronova et al. (2002) produced a limited set of radiative data for Na-like ions, calculated with their relativistic many-body codes. Some of the energies are relatively accurate, but the data does not include all the main  $n = 3$  configurations or the strongest lines.

<sup>2</sup> www.apap-network.org

May et al. (2005) [M05] presented a series of laser spectra which contained the satellite lines from AI states of Fe xv and Fe xvi and many strong Fe xvii, Fe xviii transitions. Most spectra had a lower resolution than those of Burkhalter et al. (1979). May et al. (2005) used the Hebrew University Lawrence Livermore Atomic Code (HULLAC) and the Flexible Atomic Code (FAC) to present tables of intensities, wavelenghts and identifications. It is unclear, however, which transitions would be relevant for astrophysical plasma as the laser plasma produces very different spectra.

Aggarwal & Keenan (2007) used GRASP to calculate radiative data for a limited set of  $n = 3$  states. The energies were not as accurate as those of previous authors.

Liang et al. (2008) used the  $R$ -matrix suite of codes to calculate inner-shell electron-impact excitation (EIE) rates of Fe<sup>15+</sup> for a set of  $n = 3$  states. They included Auger-plus-radiation damping and showed that earlier studies overestimated the rates. The Liang et al. (2008) EIE and the radiative data, calculated with AUTOSTRUCTURE (AS, see Badnell 2011), were included in CHIANTI version 9 (Dere et al. 2019). As the calculation focused on the scattering calculations, the AS energies were not very accurate. The CHIANTI model was complemented with AI rates calculated with AS, using the same set of configurations and the same scaling parameters for the Thomas-Fermi-Amaldi central potential, for consistency.

Graf et al. (2009) [G09] presented high-resolution (about 0.05 Å FWHM) spectra obtained in the 14.5 and 18 Å range with the LLNL EBIT. The spectra contained the strong Fe xvii and inner-shell satellites from Fe xvi. They used FAC to build an atomic model and used the relative intensities to provide a table of line identifications. No details on the atomic calculations or data were given. They also produced calculated spectra from the Cornille et al. (1994) and Phillips et al. (1997) data in a way that was not described, and concluded that the wavelenghts and relative intensities based on those previous studies were completely wrong. However, even the comparisons with the FAC model spectra was not entirely satisfactory and complicated by blending with many transitions.

Díaz et al. (2013) [D13] produced a set of accurate energies for the  $n = 3$  states, calculated with the relativistic Multireference Moller-Plesset (MR-MP) perturbation theory. For a selection of transitions, they provided wavelenghts and a comparison to those calculated by May et al. (2005) with HULLAC. They also report a table of identifications presumably based on wavelength coincidences with the observations reported by Graf et al. (2009). As Díaz et al. (2013) provided the full set of energies, it was possible to identify the correspondence with our calculations in most cases.

Beiersdorfer et al. (2012) used the Díaz et al. (2013) energies and a set of unpublished FAC calculations to revise several previous identifications of inner-shell satellites suggested by Graf et al. (2009). The authors also attempted to identify IS lines in a Chandra spectrum of Capella, although in that spectrum the lower-temperature lines are very weak, and lines from ions hotter than Fe xvii are also present.

In a follow-up paper, Beiersdorfer et al. (2014) used the Díaz et al. (2013) energies and a set of unpublished FAC calculations to indicate the predicted wavelenghts of the strongest satellites formed by DC, against the Chandra spectrum of Capella. In a similar study, more extended FAC calculations (up to  $n = 30$ ) were used by Beiersdorfer et al. (2018) to predict the intensities of  $n \geq 4$  lines formed by DC. No details were provided, although a plot in Beiersdorfer et al. (2011) on what is presumably the same calculation shows the various contributions from AI states, from which it

**Table 1.** The target electron configuration basis and orbital scaling parameters  $\lambda_{nl}$  for the structure run of the  $n = 3$  model.

| Configurations                            |    |         |    |         |
|---|----|---------|----|---------|
| $1s^2 2s^2 2p^6 3l$ ( $l=s,p,d$ )         | 1s | 1.39933 |    |         |
| $1s^2 2s^2 2p^5 3l 3l'$ ( $l, l'=s,p,d$ ) | 2s | 1.15549 | 3s | 1.13314 |
| $1s^2 2s 2p^6 3l 3l'$ ( $l, l'=s,p,d$ )   | 2p | 1.09545 | 3p | 1.09941 |
|   | 3d | 1.13123 |    |         |

appears that nearly all the flux blending the 3C line comes from AI states between  $n = 4$  and  $n = 9$ .

### 3 METHODS

Considering only dielectronic capture, the population  $N_s$  of the autoionising state  $s$  of the Na-like iron is determined by the balance between the dielectronic capture (with rate  $C^{\text{dc}}$ ), autoionisation and radiative decay to all energetically lower levels:

$$N_{\text{Ne-like}} N_e C^{\text{dc}} = N_s \left( \sum_k A_{sk}^a + \sum_{f < s} A_{sf} \right) \quad (1)$$

where  $A_{sf}$  is the transition probability to a decay to a bound state (decay rate for short),  $A_{sk}^a$  is the autoionisation rate,  $N_e$  the electron number density, and  $N_{\text{Ne-like}}$  the ground-state population of the Ne-like iron. The intensity of the satellite line decay from the state  $s$  to the bound state  $f$  is therefore proportional to

$$I_{sf}^{\text{dc}} = N_{\text{Ne-like}} N_e C^{\text{dc}} \frac{A_{sf}}{\sum_k A_{sk}^a + \sum_{f < s} A_{sf}} \quad (2)$$

By applying the Saha equation for thermodynamic equilibrium we obtain a relation between dielectronic capture and autoionisation rates and find that  $C^{\text{dc}} \propto g_s \sum_k A_{sk}^a$ , where  $g_s$  is the statistical weight of the autoionizing state. The intensity of the spectral line is therefore proportional to the factor  $F_2$ :

$$F_2 = \frac{g_s A_{sf} \sum_k A_{sk}^a}{\sum_k A_{sk}^a + \sum_{f < s} A_{sf}} = g_s A_{sf} Y \quad [s^{-1}] \quad (3)$$

which for strong lines is of the order of  $10^{13} \text{ s}^{-1}$  or higher. We provide below Tables of these factors  $F_2$ , for comparison to earlier literature, when available. We also list the ratio  $Y$ , which is an indication of how close the state is to LTE: when the AI rate  $\sum_k A_{sk}^a$  is much larger than the decay rate,  $Y \simeq 1$  and the uncertainty in the AI rate does not have a significant effect on the line intensity.

Clearly, the actual line intensity does not scale linearly with the factors  $F_2$  if the inner-shell excitation is significant. As the Na-like iron does not have metastable states for coronal densities, inner-shell excitation can only be a significant populating process for strong decays to the ground state. Generally, the intensity of the satellite line depends both on dielectronic capture and inner-shell. Our approach is to obtain the intensities of the satellite lines by solving the collisional-radiative matrix which includes both the Na- and Ne-like ions, using the IDL codes developed by one of us (GDZ) and made available to the community via CHIANTI version 9, as described in the Appendix of the paper. We adopt the total dielectronic recombination (DR) rate coefficients between the ground states of the Ne- and Na-like iron from the UK APAP network. We also include in our model level-resolved radiative recombination, with the data also from the UK APAP network.

**Table 2.** The target electron configuration basis and orbital scaling parameters  $\lambda_{nl}$  for the structure and DW runs of the  $n = 6$  model.

| Configurations  |    |         |    |         |    |         |    |         |    |         |
|---|----|---------|----|---------|----|---------|----|---------|----|---------|
| $1s^2 2s^2 2p^6 3l$ ( $l=s,p,d$ )                             | 1s | 1.39863 |    |         |    |         |    |         |    |         |
| $1s^2 2s^2 2p^6 4l$ ( $l=s,p,d,f$ )                           | 2s | 1.15549 | 3s | 1.13323 | 4s | 1.13105 | 5s | 1.12566 | 6s | 1.12792 |
| $1s^2 2s^2 2p^6 5l$ ( $l=s,p,d,f,g$ )                         | 2p | 1.09540 | 3p | 1.09919 | 4p | 1.09824 | 5p | 1.09322 | 6p | 1.09651 |
| $1s^2 2s^2 2p^6 6l$ ( $l=s,p,d,f,g,h$ )                       | 3d | 1.13139 | 4d | 1.12449 | 5d | 1.11611 | 6d | 1.11910 |    |         |
| $1s^2 2s^2 2p^5 3l n l'$ ( $l=s,p,d, n=3-6, l'=s,p,d,f,g,h$ ) | 4f | 1.22747 | 5f | 1.19739 | 6f | 1.20392 |    |         |    |         |
| $1s^2 2s 2p^6 3l n l'$ ( $l=s,p,d, n=3-6, l'=s,p,d,f,g,h$ )   | 5g | 1.33528 | 6g | 1.35001 | 6h | 1.0     |    |         |    |         |

**Table 3.** The target electron configuration basis and orbital scaling parameters  $\lambda_{nl}$  for the structure and DW runs of the  $n = 10$  model.

| Configurations   |    |         |    |         |    |         |    |         |    |         |
|--|----|---------|----|---------|----|---------|----|---------|----|---------|
| $1s^2 2s^2 2p^6 3l$ ( $l=s,p,d$ )                              | 1s | 1.40272 |    |         |    |         |    |         |    |         |
| $1s^2 2s^2 2p^6 4l$ ( $l=s,p,d,f$ )                            | 2s | 1.14452 | 3s | 1.15069 | 4s | 1.12    | 5s | 1.12052 | 6s | 1.12065 |
| $1s^2 2s^2 2p^6 5l$ ( $l=s,p,d,f,g$ )                          | 2p | 1.08489 | 3p | 1.08734 | 4p | 1.08916 | 5p | 1.08936 | 6p | 1.08962 |
| $1s^2 2s^2 2p^6 n l$ ( $n = 6 - 10, l=s,p,d,f,g,h$ )           | 3d | 1.10032 | 4d | 1.11    | 5d | 1.11005 | 6d | 1.11135 |    |         |
| $1s^2 2s^2 2p^5 3l n l'$ ( $l=s,p,d, n=3-10, l'=s,p,d,f,g,h$ ) | 4f | 1.18687 | 5f | 1.18174 | 6f | 1.18411 |    |         |    |         |
| $1s^2 2s 2p^6 3l n l'$ ( $l=s,p,d, n=3-10, l'=s,p,d,f,g,h$ )   | 5g | 1.31015 | 6g | 1.32363 | 6h | 1.10890 |    |         |    |         |

We do not attempt to model the high-density laser spectra, for a number of reasons. First, many excited states become populated and CE rates need to be included. Second, level-resolved recombination needs to be included in the model. Third, the treatment of the DR process does not include transitions among the AI states (collisional redistribution before they can relax via radiation or autoionisation), which become non-negligible for high-density plasma. Fourth, continuum lowering also needs to be modelled. Fifth, plasma conditions are such that non-Maxwellian electron distributions (NMED) and time-dependent effects naturally arise in the plasma. Sixth, modelling the relative abundance of the Ne- and Na-like ions is non-trivial. Seventh, coupling with the background radiation field in the level population modelling should be taken into account.

The radiative data,  $A_{sf}$  and  $A_{sk}^a$ , has been calculated with `AUTOSTRUCTURE`. We have run many calculations by increasing the number of configurations, as described below.

`AUTOSTRUCTURE` has a very large set of parameters and ways to run a calculation, in other words is extremely flexible. We experimented with different potentials. We tried a new development, which includes the same potential and optimization parameters as used by FAC, but it did not improve the results. We also tried semi-relaxed orbitals, where groups of configurations each have their own potential scaling parameters; and also the fully-relaxed case, where each configuration (initially) uses its own Slater-Type-Orbital potential built from its occupation numbers and, optionally, this can be iterated to self-consistency. The fully-relaxed case produced excellent energies for the lowest set of  $n = 3$  configurations, but diverged by nearly  $10,000 \text{ cm}^{-1}$  for the highest ones. At the end we used a unique set of orbitals with Thomas–Fermi scaling parameters optimized by minimizing an energy functional which included first the terms from the  $n = 2, 3$  configurations, and then iteratively those arising from higher shells.

For the calculation of the  $A_{sk}^a$  rates, we included the 6 lowest excited states in the Na-like ion. Finally, we found that the use of the kappa-averaged semi-relativistic potential improves the results.

We also added two-body non-fine-structure interactions (contact spin-spin, two-body Darwin and orbit-orbit), Breit and QED corrections.

### 3.1 CE rates

We have complemented each set of radiative data with `AUTOSTRUCTURE` Breit-Pauli distorted wave (DW) calculations with the same target. We included excitations from the ground state as well as the first four excited states, although for most astrophysical applications the population of Na-like iron is all in the ground state. The rates from excited states have been included in the models for a simple assessment of how different the relative intensities of the lines are for high-density plasmas.

Collision strengths are calculated at the same set of final scattered energies for all transitions. ‘Top-up’ for the contribution of high partial waves is done using the same Breit-Pauli methods and subroutines implemented in the R-matrix outer-region code STGF. The collision strengths were extended to high energies by interpolation using the appropriate high-energy limits, while the temperature-dependent effective collisions strength  $\Upsilon(i - j)$  (CE rate coefficients) were calculated by assuming a Maxwellian electron distribution and linear integration with the final energy of the colliding electron.

### 3.2 Other rates

When building the collisional-radiative models, we used the R-matrix CE rate coefficients and radiative data of Liang et al. (2008) for the bound states included in their model. For the Ne-like ion, we adopted the CHIANTI version 10 (Del Zanna et al. 2021) model.



#### 4 A SAMPLE OF RESULTS

We have run many AS calculations. We started with the  $n = 3$  set shown in Table 1. This set is more complete compared to that of Liang et al. (2008) (shown in Appendix), as it includes the  $2s^2 2p^5 3d^2$  configuration, not present in the earlier calculation, but that produces strong satellite lines via dielectronic capture. We have also added configurations with double excitations opening the  $2s^2$  shell. We kept the  $1s^2$  shell closed. The corresponding bound states were included.

We then increased the size by adding the  $n = 4$ ,  $n = 5$ , and  $n = 6$  orbitals and corresponding set of configurations. The  $n = 6$  model has 120 configurations and 3450 fine-structure levels. Table 2 lists the set of configurations and scaling parameters adopted for this  $n = 6$  model.

For each run we compared the energies with the experimental ones from NIST and the Díaz et al. (2013) theoretical energies. We also experimented with opening the  $1s$  shell and triple excitations, but the energies did not improve much.

The  $n = 6$  model provided theoretical energies very close to Díaz et al. (2013) and was a baseline to try and identify spectral lines using various observations, and to compare with previous identifications when possible. It provided predictions for all the observable lines. With few exceptions, relatively good agreement with observations was found.

However, considering the Beiersdorfer et al. (2011) results, a further calculation was carried out, including all the main configurations up to  $n = 10$ , to improve the predictions for the series of satellite lines blending the 3C resonance lines. The size of the model is large (288 configurations for 8886 j-resolved states) but still feasible with the CHIANTI programs. Table 3 lists the set of configurations and scaling parameters  $\lambda_{nl}$  adopted for this  $n = 10$  model. The  $\lambda_{nl}$  for  $n = 7 - 10$  have been kept equal to the  $n = 6$  ones, as it is clear that they vary little with  $n$ . It turns out that the ab-initio wavelengths are better than the  $n = 6$  model, although for most transitions up to  $n = 5$  the resulting intensities are close to those of the  $n = 6$  model.

Finally, to have an estimate of the contributions from even higher configurations, we have carried out a configuration-averaged AS calculation including the same set of configurations up to  $n = 30$ .

##### 4.1 Energies

Table 4 lists the energies of a few  $n = 3$  bound states and those of a selection of AI  $n = 3$  states. The configuration and LS labelling is from AS but is often not very meaningful. The first column lists the experimental energies which are from NIST, except a few new tentative identifications, while the second column gives the AS values obtained with the  $n = 6$  model. The following two columns list the Díaz et al. (2013) and Liang et al. (2008) values. Table A2 in the Appendix lists the energies as obtained with the  $n = 10$  model, which illustrates how little the values change with the size of the calculation. A full comparison with the Díaz et al. (2013) energies is provided in the Appendix.

Our AS energies are generally very close (within a few thousands of  $\text{cm}^{-1}$ ) to the Díaz et al. (2013) ones, especially for the states producing the strongest solar spectral lines. Note that the uncertainty in the experimental values has a similar magnitude. The comparisons with the experimental energies we have carried out indicate that the Díaz et al. (2013) are the most accurate energies across the literature. This is one of the reasons why we have in-

**Table 4.** List of the main states.

| $i$ | Conf.             | P | T           | $E_{\text{exp}}$                      | $E_{\text{AS}}$ | $E_{\text{Diaz+}}$ | $E_{\text{Liang+}}$ |
|-----|-------------------|---|-------------|---------------------------------------|-----------------|--------------------|---------------------|
| 1   | $2s^2 2p^6 3s$    | e | $^2S_{1/2}$ | 0                                     | 0               | 0                  | 0                   |
| 2   | $2s^2 2p^6 3p$    | o | $^2P_{1/2}$ | 277194                                | 277711          | 277222             | 276436              |
| 3   | $2s^2 2p^6 3p$    | o | $^2P_{3/2}$ | 298143                                | 300089          | 298167             | 296534              |
| 4   | $2s^2 2p^6 3d$    | e | $^2D_{3/2}$ | 675501                                | 676579          | 675463             | 676373              |
| 5   | $2s^2 2p^6 3d$    | e | $^2D_{5/2}$ | 678405                                | 681330          | 678372             | 679712              |
| 33  | $2s^2 2p^5 3s^2$  | o | $^2P_{3/2}$ | 5773000?                              | 5744641         | 5756556            | 5802584             |
| 34  | $2s^2 2p^5 3s^2$  | o | $^2P_{1/2}$ | 5873000?                              | 5848114         | 5857665            | 5899697             |
| 35  | $2s^2 2p^5 3s 3p$ | e | $^4S_{3/2}$ | -                                     | 5939043         | 5953391            | 5991935             |
| 36  | $2s^2 2p^5 3s 3p$ | e | $^4D_{5/2}$ | 5982000                               | 5967095         | 5980479            | 6020272             |
| 37  | $2s^2 2p^5 3s 3p$ | e | $^4D_{7/2}$ | -                                     | 5973428         | 5986775            | 6026148             |
| 38  | $2s^2 2p^5 3s 3p$ | e | $^2P_{3/2}$ | -                                     | 5974184         | 5987047            | 6027021             |
| 39  | $2s^2 2p^5 3s 3p$ | e | $^2P_{1/2}$ | 6001000                               | 5986456         | 5999543            | 6041011             |
| 40  | $2s^2 2p^5 3s 3p$ | e | $^4P_{5/2}$ | 6013000                               | 5998400         | 6011855            | 6053544             |
| 41  | $2s^2 2p^5 3s 3p$ | e | $^2D_{3/2}$ | 6013000                               | 5999767         | 6012375            | 6053898             |
| 42  | $2s^2 2p^5 3s 3p$ | e | $^2S_{1/2}$ | 6042000?                              | 6016544         | 6027754            | 6076536             |
| 43  | $2s^2 2p^5 3s 3p$ | e | $^4D_{1/2}$ | 6075000                               | 6066510         | 6077192            | 6113566             |
| 44  | $2s^2 2p^5 3s 3p$ | e | $^4P_{1/2}$ | 6089000?                              | 6072233         | 6082835            | 6128206             |
| 45  | $2s^2 2p^5 3s 3p$ | e | $^4D_{3/2}$ | 6089000                               | 6077288         | 6087509            | 6124285             |
| 46  | $2s^2 2p^5 3s 3p$ | e | $^2D_{5/2}$ | -                                     | 6087412         | 6096282            | 6141431             |
| 47  | $2s^2 2p^5 3s 3p$ | e | $^4P_{3/2}$ | 6096000                               | 6089389         | 6100268            | 6138528             |
| 48  | $2s^2 2p^5 3s 3p$ | e | $^2D_{5/2}$ | 6110000                               | 6098693         | 6108077            | 6147237             |
| 49  | $2s^2 2p^5 3s 3p$ | e | $^2P_{3/2}$ | 6129000?                              | 6105380         | 6113831            | 6157761             |
| 50  | $2s^2 2p^5 3s 3p$ | e | $^2P_{1/2}$ | -                                     | 6178837         | 6182346            | 6229457             |
| 51  | $2s^2 2p^5 3s 3p$ | e | $^2D_{3/2}$ | 6217000?                              | 6195854         | 6201702            | 6244142             |
| 52  | $2s^2 2p^5 3s 3p$ | e | $^2S_{1/2}$ | 6267000?                              | 6252510         | 6245187            | 6313279             |
| 67  | $2s^2 2p^5 3s 3d$ | o | $^4P_{5/2}$ | 6393000                               | 6379612         | 6390567            | 6440048             |
| 73  | $2s^2 2p^5 3s 3d$ | o | $^4F_{5/2}$ | 6406000                               | 6394429         | 6404701            | 6453145             |
| 74  | $2s^2 2p^5 3p^2$  | o | $^2P_{3/2}$ | -                                     | 6397961         | 6406003            | 6469670             |
| 75  | $2s^2 2p^5 3s 3d$ | o | $^2D_{3/2}$ | 6419000                               | 6405385         | 6415660            | 6464402             |
| 76  | $2s^2 2p^5 3p^2$  | o | $^2D_{3/2}$ | -                                     | 6413008         | 6422064            | 6455698             |
| 77  | $2s^2 2p^5 3s 3d$ | o | $^4D_{7/2}$ | 6422000                               | 6413123         | 6421329            | 6471649             |
| 78  | $2s^2 2p^5 3s 3d$ | o | $^2P_{1/2}$ | 6423000                               | 6415027         | 6423498            | 6464730             |
| 79  | $2s^2 2p^5 3s 3d$ | o | $^2F_{5/2}$ | 6425000                               | 6415181         | 6423578            | 6476262             |
| 80  | $2s^2 2p^5 3p^2$  | o | $^2D_{5/2}$ | -                                     | 6417371         | 6425339            | 6474699             |
| 81  | $2s^2 2p^5 3s 3d$ | o | $^2P_{3/2}$ | <del>6436000</del><br><b>6444100?</b> | 6436676         | 6443091            | 6498398             |
| 82  | $2s^2 2p^5 3s 3d$ | o | $^4D_{1/2}$ | -                                     | 6447867         | 6455202            | 6506414             |
| 83  | $2s^2 2p^5 3s 3d$ | o | $^4D_{3/2}$ | <del>6473000</del>                    | 6476481         | 6483365            | 6536053             |
| 84  | $2s^2 2p^5 3s 3d$ | o | $^2F_{7/2}$ | <del>6445000</del>                    | 6480673         | 6485011            | 6546990             |
| 85  | $2s^2 2p^5 3s 3d$ | o | $^4F_{3/2}$ | 6502000                               | 6493786         | 6502061            | 6547383             |
| 86  | $2s^2 2p^5 3s 3d$ | o | $^2D_{5/2}$ | <del>6464000</del>                    | 6495941         | 6501608            | 6549706             |
| 87  | $2s^2 2p^5 3s 3d$ | o | $^4D_{5/2}$ | 6502000                               | 6496993         | 6504077            | 6555370             |

$E_{\text{exp}}$  gives the NIST experimental energies, except the those in bold which are our tentative values.  $E_{\text{AS}}$  are our ab-initio AS energies with the  $n = 6$  model.  $E_{\text{Diaz+}}$  are the energies from Díaz et al. (2013) while  $E_{\text{Liang+}}$  are the AS ones from Liang et al. (2008).

cluded them in the Table. The other is that the authors provided the full set of states so we could match them against ours with some confidence.

Our energies predict the  $2p^5 3s 3p \ ^4D_{7/2}$  (level No.81) -  $2p^5 3s 3d \ ^4F_{9/2}$  (level No.112) transition, identified with a line at  $248.36 \pm 0.05 \text{ \AA}$  by Jupen et al. (1988), to be at  $245.9 \text{ \AA}$ , while the Díaz et al. (2013) energies predict  $248.5 \text{ \AA}$ .

Table 4 also clearly shows that the Liang et al. (2008) energies differ by a significant amount, about  $40,000 \text{ cm}^{-1}$ . This is the reason why the mixing of the states and ultimately the rates obtained

**Table 4.** Contd

| $i$ | Conf.   | P | T                             | $E_{\text{NIST}}$                     | $E_{\text{AS}}$ | $E_{\text{Diaz+}}$ | $E_{\text{Liang+}}$ |
|-----|---|---|-------------------------------|---------------------------------------|-----------------|--------------------|---------------------|
| 88  | 2s <sup>2</sup> 2p <sup>5</sup> 3p <sup>2</sup> | o | <sup>2</sup> P <sub>1/2</sub> | -                                     | 6504938         | 6508883            | 6566725             |
| 89  | 2s <sup>2</sup> 2p <sup>5</sup> 3s 3d           | o | <sup>2</sup> D <sub>5/2</sub> | 6516000                               | 6508973         | 6514575            | 6569938             |
| 90  | 2s <sup>2</sup> 2p <sup>5</sup> 3s 3d           | o | <sup>2</sup> F <sub>7/2</sub> | 6517000                               | 6509407         | 6514871            | 6561652             |
| 91  | 2s <sup>2</sup> 2p <sup>5</sup> 3p <sup>2</sup> | o | <sup>2</sup> P <sub>1/2</sub> | -                                     | 6511585         | 6514341            | 6579688             |
| 92  | 2s <sup>2</sup> 2p <sup>5</sup> 3p <sup>2</sup> | o | <sup>2</sup> P <sub>3/2</sub> | -                                     | 6528784         | 6531608            | 6592253             |
| 93  | 2s <sup>2</sup> 2p <sup>5</sup> 3s 3d           | o | <sup>2</sup> D <sub>3/2</sub> | <del>6530000</del><br><b>6553500?</b> | 6549199         | 6550184            | 6611638             |
| 94  | 2s <sup>2</sup> 2p <sup>5</sup> 3s 3d           | o | <sup>2</sup> P <sub>1/2</sub> | 6574000                               | 6575409         | 6573657            | 6644694             |
| 95  | 2s <sup>2</sup> 2p <sup>5</sup> 3p 3d           | e | <sup>4</sup> D <sub>1/2</sub> | -                                     | 6586884         | 6601400            | 6646599             |
| 96  | 2s <sup>2</sup> 2p <sup>5</sup> 3s 3d           | o | <sup>2</sup> F <sub>5/2</sub> | <del>6556000</del>                    | 6591507         | 6593543            | 6651977             |
| 97  | 2s <sup>2</sup> 2p <sup>5</sup> 3p 3d           | e | <sup>4</sup> D <sub>3/2</sub> | -                                     | 6595119         | 6608991            | 6654887             |
| 98  | 2s <sup>2</sup> 2p <sup>5</sup> 3p 3d           | e | <sup>4</sup> D <sub>5/2</sub> | -                                     | 6607993         | 6620899            | 6667902             |
| 99  | 2s <sup>2</sup> 2p <sup>5</sup> 3s 3d           | o | <sup>2</sup> P <sub>3/2</sub> | <del>6595000</del><br><b>6620000?</b> | 6617260         | 6616740            | 6686516             |
| 151 | 2s <sup>2</sup> 2p <sup>5</sup> 3p 3d           | e | <sup>2</sup> D <sub>3/2</sub> | <b>6831000?</b>                       | 6833056         | 6831282            | 6894915             |
| 152 | 2s <sup>2</sup> 2p <sup>5</sup> 3p 3d           | e | <sup>2</sup> D <sub>5/2</sub> | <b>6837100?</b>                       | 6837436         | 6838045            | 6893483             |
| 191 | 2s <sup>2</sup> 2p <sup>5</sup> 3d <sup>2</sup> | o | <sup>2</sup> G <sub>7/2</sub> | <b>7135000?</b>                       | 7130233         | 7134361            | -                   |
| 192 | 2s <sup>2</sup> 2p <sup>5</sup> 3d <sup>2</sup> | o | <sup>4</sup> F <sub>5/2</sub> | -                                     | 7136863         | 7142053            | -                   |
| 193 | 2s 2p <sup>6</sup> 3s 3p                        | o | <sup>2</sup> P <sub>3/2</sub> | -                                     | 7138849         | 7128949            | -                   |
| 200 | 2s <sup>2</sup> 2p <sup>5</sup> 3d <sup>2</sup> | o | <sup>2</sup> F <sub>5/2</sub> | <b>7180800?</b>                       | 7183602         | 7186088            | -                   |
| 201 | 2s <sup>2</sup> 2p <sup>5</sup> 3d <sup>2</sup> | o | <sup>2</sup> F <sub>5/2</sub> | <b>7191000?</b>                       | 7188617         | 7193832            | -                   |
| 210 | 2s <sup>2</sup> 2p <sup>5</sup> 3d <sup>2</sup> | o | <sup>2</sup> F <sub>7/2</sub> | <b>7236000?</b>                       | 7241831         | 7242818            | -                   |
| 211 | 2s <sup>2</sup> 2p <sup>5</sup> 3d <sup>2</sup> | o | <sup>2</sup> D <sub>5/2</sub> | <b>7240000?</b>                       | 7251131         | 7246119            | -                   |
| 212 | 2s <sup>2</sup> 2p <sup>5</sup> 3d <sup>2</sup> | o | <sup>2</sup> D <sub>3/2</sub> | -                                     | 7257952         | 7253388            | -                   |
| 213 | 2s <sup>2</sup> 2p <sup>5</sup> 3d <sup>2</sup> | o | <sup>2</sup> P <sub>3/2</sub> | <b>7266000?</b>                       | 7269242         | 7263947            | -                   |

with the Liang et al. (2008) model are sometimes quite different than those we have calculated, as shown below.

Table 4 also shows that in several cases the NIST energies must be incorrect, not only because of the large departures from the Díaz et al. (2013) (or our) values, but also because the intensities of their decays do not match solar observations, as briefly outlined below. We have highlighted the main ones, but in several other cases, where a question mark is added, the NIST values might also be wrong.

Unfortunately, we have a circular problem: the published structure calculations provide different wavelengths and intensities, hence different identifications. As pointed out by Burkhalter et al. (1979), studies along the sequence do not help. For a few states producing the strongest lines, we have provided tentative new energies and used them for the comparisons to observations. Details are provided below. We have not attempted to apply semi-empirical corrections to the calculations as implemented within AS, and which would improve the results. They could be applied in the future, once the main transitions will be firmly established with new laboratory and solar spectra.

## 4.2 Radiative data

Table 5 shows as an example the CHIANTI radiative data, which were obtained from the Liang et al. (2008)  $n = 3$  target and those we have calculated with the more extended  $n = 3$  sets of configurations and different scaling parameters of Table 1. Only transitions from the lowest AI states and with an intensity factor  $F_2$  larger than  $5 \times 10^{11}$  are shown. Note that typical values of  $F_2$  of observed lines in astrophysical spectra are  $10^{13}$  or higher, although the large num-

ber of weak transitions within short wavelength intervals means that weaker transitions can also be significant. We have removed from the model transitions with branching ratios less than  $10^{-5}$  but the total number of satellite lines, all within 11–18 Å, is over 700 000.

We can see that differences of a factor of two in the  $F_2$  values are common, although some transitions, indicated in the last column, are actually mainly formed by IS, and not DC, hence the  $F_2$  value is not related to the actual intensity of the line. Sometimes the differences are related to the decay rate, sometimes with the AI rate.

There are also cases as the first transition in the Table where the decay rate is similar but the AI rate is different by nearly a factor of three. By running many calculations, we found that even small changes in the CI expansion or the scaling parameters can have a large effect on the AI rates, easily by an order of magnitude. On the other hand, the radiative rates are generally less affected. Almost all the AI states are completely mixed, and any small change in the relative energies can have a large effect on the mixing and on the AI rates. The fact that the radiative data are often less affected is due to the different sensitivity to the short and long-range parts of the wavefunctions.

We are not aware that this important issue has been highlighted in the literature. On the other hand, it is also worth pointing out that a large uncertainty in the AI rate does not affect the line intensity when the ratio  $Y$  is close to unity, as the AI state is in LTE (AI rate dominant over the decay rate). We have highlighted in the last column the cases where  $Y$  is much lower than 1 and the calculated AI rates vary significantly.

To validate the AS AI rates, we have run a calculation with the  $n = 3$  set, switched off the corrections for the two-body non-fine-structure interactions, and run the Breit-Pauli  $R$ -matrix (BPRM) suite of codes with a relatively simple Ne-like target (4 configurations). We used the Quigley and Berrington method (Quigley & Berrington 1996; Quigley et al. 1998) to locate resonances and get their widths. This process is time consuming, so only a sample of values are shown. We are not aware of any such comparison presented in the literature. Table 5 shows the ratio  $R$  between the AS AI rates and those calculated from the widths of the resonances.

The comparison with the  $R$ -matrix AI rates is reassuring, with typical differences for the stronger transitions of 10–30%. However, in a few cases large differences are present. We have verified that they occur when two states that are mixing are very close in energy. Generally, the  $R$ -matrix energies are quite different from the AS values, even using the same target, so the mixing of states is often quite different.

Table 6 lists all the main  $n = 3$  transitions formed by dielectronic capture, having an intensity factor  $F_2$  larger than  $10^{13}$ . The results are from the  $n = 6$  model. We compare our ab-initio wavelengths and  $F_2$  values with those from Phillips et al. (1997), finding in some cases significant differences. We also compare our  $F_2$  values with those from Cornille et al. (1994), finding a large scatter of values. We list a question mark when the level matching is unclear. We believe that the main differences in the  $F_2$  values are due to the different AI rates used for the three calculations. We list in the last columns the AI rates from two of our calculations, and those calculated with Cowan’s code by Bruch et al. (1998) and with YODA by Nilsen (1989). We see large discrepancies even for strong transitions. The most important cases, highlighted with an asterisk in the last column, are when the ratio  $Y$  is far from unity. However, with a few exceptions, the scatter of values is within 30%.

**Table 5.** List of the main transitions from the lowest states formed by dielectronic capture ( $n=3$  models). F2 values, as well as  $A_{ji}$  and AI rates are in  $10^{13} \text{ s}^{-1}$ .

| $j$ | $i$ | $C_j$                           | $T_j$                         | $C_i$ | $T_i$                         | $\lambda$<br>Å | $F_2$<br>v9 | $A_{ji}$<br>V9 | $F_2$<br>$n = 3$ | $Y$<br>$n = 3$ | $A_{ji}$<br>$n = 3$ | AI<br>v9 | AI<br>$n = 3$ | R    |      |
|-----|-----|---------------------------------|-------------------------------|-------|-------------------------------|----------------|-------------|----------------|------------------|----------------|---------------------|----------|---------------|------|------|
| 33  | 1   | 2p <sup>5</sup> 3s <sup>2</sup> | <sup>2</sup> P <sub>3/2</sub> | 3s    | <sup>2</sup> S <sub>1/2</sub> | 17.322         | 0.17        | 0.064          | 0.25             | 0.77           | 0.082               | 0.12     | 0.28          | 1.10 | *    |
| 40  | 3   | 2p <sup>5</sup> 3s 3p           | <sup>4</sup> P <sub>5/2</sub> | 3p    | <sup>2</sup> P <sub>3/2</sub> | 17.498         | 0.09        | 0.031          | 0.08             | 0.35           | 0.037               | 0.027    | 0.020         | 0.53 | *    |
| 50  | 3   | 2p <sup>5</sup> 3s 3p           | <sup>2</sup> P <sub>1/2</sub> | 3p    | <sup>2</sup> P <sub>3/2</sub> | 16.855         | 0.15        | 0.075          | 0.16             | 0.98           | 0.083               | 3.2      | 4.3           | 1.31 |      |
| 51  | 3   | 2p <sup>5</sup> 3s 3p           | <sup>2</sup> D <sub>3/2</sub> | 3p    | <sup>2</sup> P <sub>3/2</sub> | 16.895         | 0.09        | 0.031          | 0.09             | 0.52           | 0.042               | 0.12     | 0.059         | 1.41 |      |
| 73  | 4   | 2p <sup>5</sup> 3s 3d           | <sup>4</sup> F <sub>5/2</sub> | 3d    | <sup>2</sup> D <sub>3/2</sub> | 17.450         | 0.11        | 0.022          | 0.14             | 0.61           | 0.037               | 0.13     | 0.068         | 0.68 | *    |
| 78  | 5   | 2p <sup>5</sup> 3s 3d           | <sup>4</sup> D <sub>7/2</sub> | 3d    | <sup>2</sup> D <sub>5/2</sub> | 17.411         | 0.16        | 0.023          | 0.21             | 0.72           | 0.037               | 0.18     | 0.098         | 0.70 | *    |
| 79  | 5   | 2p <sup>5</sup> 3s 3d           | <sup>2</sup> F <sub>5/2</sub> | 3d    | <sup>2</sup> D <sub>5/2</sub> | 17.402         | 0.14        | 0.028          | 0.09             | 0.56           | 0.028               | 0.26     | 0.068         | 0.01 | *    |
| 79  | 4   | 2p <sup>5</sup> 3s 3d           | <sup>2</sup> F <sub>5/2</sub> | 3d    | <sup>2</sup> D <sub>3/2</sub> | 17.393         | 0.12        | 0.023          | 0.07             | 0.56           | 0.023               |          |               |      |      |
| 80  | 4   | 2p <sup>5</sup> 3s 3d           | <sup>2</sup> P <sub>1/2</sub> | 3d    | <sup>2</sup> D <sub>3/2</sub> | 17.399         | 0.07        | 0.039          | 0.12             | 0.89           | 0.069               | 2.4      | 1.1           | 1.70 |      |
| 80  | 1   | 2p <sup>5</sup> 3s 3d           | <sup>2</sup> P <sub>1/2</sub> | 3s    | <sup>2</sup> S <sub>1/2</sub> | 15.569         | 0.10        | 0.052          | 0.11             |                | 0.063               |          |               |      |      |
| 81  | 5   | 2p <sup>5</sup> 3s 3d           | <sup>2</sup> P <sub>3/2</sub> | 3d    | <sup>2</sup> D <sub>5/2</sub> | 17.368         | 0.08        | 0.038          | 0.13             | 0.43           | 0.078               | 0.40     | 0.30          | 1.86 | *    |
| 81  | 1   | 2p <sup>5</sup> 3s 3d           | <sup>2</sup> P <sub>3/2</sub> | 3s    | <sup>2</sup> S <sub>1/2</sub> | 15.536         | 0.62        | 0.28           | 0.54             |                | 0.31                |          |               |      | * IS |
| 82  | 1   | 2p <sup>5</sup> 3s 3d           | <sup>4</sup> D <sub>1/2</sub> | 3s    | <sup>2</sup> S <sub>1/2</sub> | 15.369         | 0.62        | 0.32           | 0.76             | 0.95           | 0.40                | 10       | 7.9           | 1.12 |      |
| 83  | 1   | 2p <sup>5</sup> 3s 3d           | <sup>4</sup> D <sub>3/2</sub> | 3s    | <sup>2</sup> S <sub>1/2</sub> | 15.449         | 0.40        | 0.10           | 0.67             | 0.97           | 0.17                | 8.3      | 7.9           | 1.22 |      |
| 84  | 5   | 2p <sup>5</sup> 3s 3d           | <sup>2</sup> F <sub>7/2</sub> | 3d    | <sup>2</sup> D <sub>5/2</sub> | 17.341         | 0.10        | 0.013          | 0.18             | 0.96           | 0.023               | 0.59     | 0.59          | 1.15 |      |
| 85  | 4   | 2p <sup>5</sup> 3s 3d           | <sup>4</sup> F <sub>3/2</sub> | 3d    | <sup>2</sup> D <sub>3/2</sub> | 17.163         | 0.12        | 0.03           | 0.20             | 0.94           | 0.053               | 2.2      | 1.1           | 1.40 |      |
| 85  | 1   | 2p <sup>5</sup> 3s 3d           | <sup>4</sup> F <sub>3/2</sub> | 3s    | <sup>2</sup> S <sub>1/2</sub> | 15.380         | 0.11        | 0.029          | 0.07             |                | 0.019               |          |               |      |      |
| 88  | 5   | 2p <sup>5</sup> 3s 3d           | <sup>2</sup> F <sub>7/2</sub> | 3d    | <sup>2</sup> D <sub>5/2</sub> | 17.127         | 0.27        | 0.039          | 0.32             | 0.61           | 0.065               | 0.24     | 0.11          | 0.79 | *    |
| 90  | 5   | 2p <sup>5</sup> 3s 3d           | <sup>2</sup> D <sub>5/2</sub> | 3d    | <sup>2</sup> D <sub>5/2</sub> | 17.130         | 0.12        | 0.031          | 0.13             | 0.23           | 0.097               | 0.099    | 0.043         | 0.81 | *    |
| 90  | 4   | 2p <sup>5</sup> 3s 3d           | <sup>2</sup> D <sub>5/2</sub> | 3d    | <sup>2</sup> D <sub>3/2</sub> | 17.122         | 0.08        | 0.020          | 0.06             |                | 0.047               |          |               |      |      |
| 92  | 4   | 2p <sup>5</sup> 3p <sup>2</sup> | <sup>2</sup> P <sub>3/2</sub> | 3d    | <sup>2</sup> D <sub>3/2</sub> | 16.904         | 0.07        | 0.017          | 0.12             | 1.0            | 0.030               | 34       | 35            | 0.84 |      |
| 92  | 1   | 2p <sup>5</sup> 3p <sup>2</sup> | <sup>2</sup> P <sub>3/2</sub> | 3s    | <sup>2</sup> S <sub>1/2</sub> | 15.169         | 0.75        | 0.019          | 0.02             |                | 0.004               |          |               |      |      |
| 93  | 1   | 2p <sup>5</sup> 3s 3d           | <sup>2</sup> D <sub>3/2</sub> | 3s    | <sup>2</sup> S <sub>1/2</sub> | 15.314         | 0.64        | 1.3            | 4.3              | 0.69           | 1.6                 | 0.19     | 3.6           | 0.56 | * IS |
| 94  | 1   | 2p <sup>5</sup> 3s 3d           | <sup>2</sup> P <sub>1/2</sub> | 3s    | <sup>2</sup> S <sub>1/2</sub> | 15.211         | 1.10        | 2.5            | 0.11             | 0.02           | 2.6                 | 0.71     | 0.059         | 0.04 | * IS |
| 96  | 5   | 2p <sup>5</sup> 3s 3d           | <sup>2</sup> F <sub>5/2</sub> | 3d    | <sup>2</sup> D <sub>5/2</sub> | 17.014         | 0.07        | 0.013          | 0.19             | 0.90           | 0.036               | 0.33     | 0.41          | 0.99 |      |
| 102 | 1   | 2p <sup>5</sup> 3s 3d           | <sup>2</sup> P <sub>3/2</sub> | 3s    | <sup>2</sup> S <sub>1/2</sub> | 15.163         | 3.6         | 1.1            | 3.4              | 0.84           | 1.0                 | 5.3      | 5.6           | 0.60 | * IS |

The first columns give the upper  $j$  and lower  $i$  level number, the main configurations from the CHIANTI v.9  $n=3$  model and the CHIANTI v.9 wavelength (Å) of the transition. Column 5 gives the F2 value (only the strongest lines with values higher than  $5 \times 10^{11}$  are shown. Note that single observed lines have typical values higher than  $10^{13}$ ). The following columns show the CHIANTI v.9 A-values and those with our improved  $n = 3$  model, and the total AI rates from the autoionizing state. The final column gives R, the ratio between the AI rate as calculated with the same improved  $n = 3$  model and with the  $R$ -matrix codes.

### 4.3 CE rates - DW vs. $R$ -matrix

One important issue is whether the DW approach provides accurate CE rates, compared to those obtained with the  $R$ -matrix codes. As the effect of the resonances is small for the AI states, also considering the resonances is small for the AI states, one would expect that the DW rates are accurate enough even for the  $n = 3$  states.

We found that variations of the order of 20-30% in the CE rates calculated with different targets are common, but are mostly related to the variations in the oscillator strengths of each set of calculations, as one would expect.

We have compared the DW cross-sections and rate coefficients for key transitions formed by inner-shell excitation with those calculated by Liang et al. (2008) using the  $R$ -matrix codes and radiation damping, finding overall very good agreement. Figure 1 shows a comparison of rate coefficients for the strongest transitions, calculated with the  $n = 6$  model. The minor differences are related to the different  $gf$  values, which are listed in the plot.

## 5 COMPARISON WITH SOLAR OBSERVATIONS

Clearly, in any laboratory or astrophysical spectra, the satellite lines will always be blended with lines from the Ne-like iron and other ions. As the Na-like abundance peaks around 2 MK in ionization

equilibrium, the best spectra would be those of 2 MK plasma. Unfortunately, except for the very low resolution ones of MaGIXS, no solar spectra of 2 MK plasma around 15 Å exist.

Most of the spectra in this spectral region are of flares or active regions where the peak temperature is at least 3 MK. Chandra spectra of cool stars exist but do not have resolution and signal-to-noise comparable to solar spectra.

The best astrophysical spectrum of the 15–17 Å range, with the Fe xvii lines and their satellites was taken by a Skylark sounding rocket on 30 Nov. 1971, with Bragg crystal spectrometers built by the University of Leicester (UK) under the supervision of Ken Pounds, pioneer of X-ray astronomy. The spectrum was of a quiescent active region and is high-resolution as the instrumental FWHM was about 0.025 Å. Weak lines were measured, and the wavelength and radiometric calibration was excellent. Details and a Table of wavelengths and fluxes are found in (hereafter P75 Parkinson 1975). Some results from analyses of this spectrum were published by Del Zanna (2011) and Del Zanna & Mason (2014), where the P75 fluxes were converted to radiances.

The P75 spectra in the plots of the paper appear noisy, and do not clearly show all the measured line intensities listed in the published Table. On the other hand, there are weak features in the spectra that are not listed in the Table. To help the atomic data benchmarking procedure, we have created a reconstructed P75 spectrum

**Table 6.** List of the  $n = 3$  transitions formed by dielectronic capture with strongest intensity factor  $F_2$  ( $n=6$  model).

| $j$ | $i$ | $C_j$   | $T_j$  | $C_i$ | $T_i$                         | $\lambda$<br>(Å) | $\lambda(P)$<br>(Å) | $F_2$ | $Y$  | $F_2(P)$ | $F_2(C)$ | $A_{ji}$<br>$n = 6$ | AI<br>$n = 6$ | AI<br>$n = 3$ | AI<br>B98 | AI<br>N86 |    |
|-----|-----|---|--|-------|-------------------------------|------------------|---------------------|-------|------|----------|----------|---------------------|---------------|---------------|-----------|-----------|----|
| 82  | 1   | 2s <sup>2</sup> 2p <sup>5</sup> 3s 3d           | <sup>4</sup> D <sub>1/2</sub>                  | 3s    | <sup>2</sup> S <sub>1/2</sub> | 15.509           | 15.181?             | 0.72  | 0.95 | 1.5 ?    | 1.1 ?    | 0.38                | 7.1           | 7.9           | 7.9       | 8.6       |    |
| 93  | 1   | 2s <sup>2</sup> 2p <sup>5</sup> 3s 3d           | <sup>2</sup> D[ <sup>2</sup> P] <sub>3/2</sub> | 3s    | <sup>2</sup> S <sub>1/2</sub> | 15.269           |                     | 3.9   | 0.67 |          |          | 1.5                 | 3.1           | 3.6           | 2.0       | 5.0       | IS |
| 99  | 1   | 2s <sup>2</sup> 2p <sup>5</sup> 3s 3d           | <sup>2</sup> P <sub>3/2</sub>                  | 3s    | <sup>2</sup> S <sub>1/2</sub> | 15.112           | 15.148              | 3.3   | 0.84 | 2.4      | 3.8      | 0.99                | 5.5           | 5.6           | 3.3       | 4.2       | IS |
| 140 | 3   | 2s <sup>2</sup> 2p <sup>5</sup> 3p 3d           | <sup>4</sup> P[ <sup>2</sup> D] <sub>5/2</sub> | 3p    | <sup>2</sup> P <sub>3/2</sub> | 15.432           |                     | 1.1   | 0.98 |          |          | 0.18                | 7.4           | 5.7           | 5.2       | 4.5       |    |
| 143 | 3   | 2s <sup>2</sup> 2p <sup>5</sup> 3p 3d           | <sup>2</sup> D <sub>5/2</sub>                  | 3p    | <sup>2</sup> P <sub>3/2</sub> | 15.399           | 15.029?             | 0.58  | 0.83 | 1.1?     |          | 0.12                | 0.58          | 0.6           | 4.8e-3    | 0.013     | *  |
| 151 | 2   | 2s <sup>2</sup> 2p <sup>5</sup> 3p 3d           | <sup>2</sup> D <sub>3/2</sub>                  | 3p    | <sup>2</sup> P <sub>1/2</sub> | 15.255           | 15.221?             | 7.3   | 0.88 | 8.2?     | 8.1?     | 2.1                 | 16            | 13            | 11        | 11        |    |
| 152 | 3   | 2s <sup>2</sup> 2p <sup>5</sup> 3p 3d           | <sup>2</sup> D <sub>5/2</sub>                  | 3p    | <sup>2</sup> P <sub>3/2</sub> | 15.297           | 15.138?             | 4.8   | 0.85 | 3.0      |          | 0.95                | 5.3           | 4.8           | 3.9       | 4.2       |    |
| 153 | 2   | 2s <sup>2</sup> 2p <sup>5</sup> 3p 3d           | <sup>2</sup> P <sub>1/2</sub>                  | 3p    | <sup>2</sup> P <sub>1/2</sub> | 15.237           | 15.212              | 1.7   | 0.56 | 1.8      | 1.7      | 1.5                 | 2.0           | 1.9           | 2.3       | 2.5       | *  |
| 154 | 3   | 2s <sup>2</sup> 2p <sup>5</sup> 3p 3d           | <sup>2</sup> P <sub>3/2</sub>                  | 3p    | <sup>2</sup> P <sub>3/2</sub> | 15.245           | 15.146?             | 0.29  | 0.04 | 2.8 ?    | 2.4 ?    | 1.8                 | 0.077         | 0.025         | 8e-4      | 4.8e-3    | *  |
| 156 | 3   | 2s <sup>2</sup> 2p <sup>5</sup> 3p 3d           | <sup>2</sup> P <sub>1/2</sub>                  | 3p    | <sup>2</sup> P <sub>3/2</sub> | 15.190           |                     | 1.5   | 0.43 |          |          | 1.7                 | 1.3           | 0.8           | 2.1       | 1.8       | *  |
| 159 | 3   | 2s <sup>2</sup> 2p <sup>5</sup> 3p 3d           | <sup>2</sup> P[ <sup>2</sup> D] <sub>3/2</sub> | 3p    | <sup>2</sup> P <sub>3/2</sub> | 15.157           |                     | 1.9   | 0.91 |          |          | 0.5                 | 5.7           | 6.0           | 7.2       | 5.7       |    |
| 160 | 2   | 2s <sup>2</sup> 2p <sup>5</sup> 3p 3d           | <sup>2</sup> S <sub>1/2</sub>                  | 3p    | <sup>2</sup> P <sub>1/2</sub> | 15.066           | 15.069              | 1.1   | 0.76 | 1.4      | 1.4      | 0.7                 | 3.1           | 2.9           | 4.2       | 4.0       | *  |
| 188 | 4   | 2s <sup>2</sup> 2p <sup>5</sup> 3d <sup>2</sup> | <sup>4</sup> G <sub>5/2</sub>                  | 3d    | <sup>2</sup> D <sub>3/2</sub> | 15.525           | 15.496 ?            | 1.8   | 0.97 | 1.4      | 1.4      | 0.31                | 14            | 14            | 16        | 14        |    |
| 188 | 5   | 2s <sup>2</sup> 2p <sup>5</sup> 3d <sup>2</sup> | <sup>4</sup> G <sub>5/2</sub>                  | 3d    | <sup>2</sup> D <sub>5/2</sub> | 15.536           | 15.464 ?            | 0.53  |      | 1.1      |          | 0.09                |               |               |           |           |    |
| 191 | 5   | 2s <sup>2</sup> 2p <sup>5</sup> 3d <sup>2</sup> | <sup>2</sup> G <sub>7/2</sub>                  | 3d    | <sup>2</sup> D <sub>5/2</sub> | 15.507           | 15.474              | 2.1   | 0.97 | 2.2      | 1.7      | 0.27                | 8.0           | 7.7           | 9.2       | 8.5       |    |
| 192 | 5   | 2s <sup>2</sup> 2p <sup>5</sup> 3d <sup>2</sup> | <sup>4</sup> F <sub>5/2</sub>                  | 3d    | <sup>2</sup> D <sub>5/2</sub> | 15.491           |                     | 1.0   | 0.67 |          |          | 0.25                | 0.8           | 1.0           | 1.2       | 1.3       |    |
| 193 | 1   | 2s 2p <sup>6</sup> 3s 3p                        | <sup>2</sup> P <sub>3/2</sub>                  | 3s    | <sup>2</sup> S <sub>1/2</sub> | 14.008           |                     | 1.2   | 0.95 |          |          | 0.31                | 6.7           | 6.0           | 7.2       | 8.2       |    |
| 196 | 4   | 2s <sup>2</sup> 2p <sup>5</sup> 3d <sup>2</sup> | <sup>4</sup> D <sub>1/2</sub>                  | 3d    | <sup>2</sup> D <sub>3/2</sub> | 15.424           | 15.407              | 0.90  | 0.63 | 1.1      |          | 0.7                 | 1.2           | 0.73          | 1.5       | 1.1       | *  |
| 198 | 5   | 2s <sup>2</sup> 2p <sup>5</sup> 3d <sup>2</sup> | <sup>2</sup> P[ <sup>4</sup> S] <sub>3/2</sub> | 3d    | <sup>2</sup> D <sub>5/2</sub> | 15.385           | 15.376              | 0.85  | 0.82 | 1.0      |          | 0.26                | 1.2           | 0.67          | 1.4       | 0.9       | *  |
| 199 | 5   | 2s <sup>2</sup> 2p <sup>5</sup> 3d <sup>2</sup> | <sup>2</sup> F <sub>7/2</sub>                  | 3d    | <sup>2</sup> D <sub>5/2</sub> | 15.382           | 15.353              | 1.8   | 0.93 | 2.1      | 2.0      | 0.24                | 3.4           | 4.2           | 4.5       | 5.2       |    |
| 200 | 4   | 2s <sup>2</sup> 2p <sup>5</sup> 3d <sup>2</sup> | <sup>2</sup> F[ <sup>2</sup> D] <sub>5/2</sub> | 3d    | <sup>2</sup> D <sub>3/2</sub> | 15.368           | 15.329              | 2.8   | 0.88 | 7.9      | 8.8      | 0.5                 | 5.1           | 3.7           | 6.3       | 2.7       | *  |
| 200 | 5   | 2s <sup>2</sup> 2p <sup>5</sup> 3d <sup>2</sup> | <sup>2</sup> F <sub>5/2</sub>                  | 3d    | <sup>2</sup> D <sub>5/2</sub> | 15.379           |                     | 1.1   |      |          |          | 0.2                 | 5.1           |               |           |           |    |
| 201 | 4   | 2s <sup>2</sup> 2p <sup>5</sup> 3d <sup>2</sup> | <sup>2</sup> F <sub>5/2</sub>                  | 3d    | <sup>2</sup> D <sub>3/2</sub> | 15.356           |                     | 5.5   | 0.97 |          |          | 0.9                 | 32            | 34            | 6.4       | 39        |    |
| 209 | 4   | 2s <sup>2</sup> 2p <sup>5</sup> 3d <sup>2</sup> | <sup>2</sup> P <sub>1/2</sub>                  | 3d    | <sup>2</sup> D <sub>3/2</sub> | 15.240           | 15.227              | 1.4   | 0.52 | 1.7      | 2.0      | 1.3                 | 1.5           | 1.6           | 1.3       | *         |    |
| 210 | 5   | 2s <sup>2</sup> 2p <sup>5</sup> 3d <sup>2</sup> | <sup>2</sup> F <sub>7/2</sub>                  | 3d    | <sup>2</sup> D <sub>5/2</sub> | 15.243           | 15.205              | 10    | 0.96 | 11       | 11       | 1.3                 | 35            | 36            | 42        | 39        |    |
| 211 | 5   | 2s <sup>2</sup> 2p <sup>5</sup> 3d <sup>2</sup> | <sup>2</sup> D <sub>5/2</sub>                  | 3d    | <sup>2</sup> D <sub>5/2</sub> | 15.221           | 15.194              | 2.8   | 0.19 | 3.8      | 3.3      | 2.5                 | 0.59          | 0.61          | 0.66      | 0.62      |    |
| 212 | 4   | 2s <sup>2</sup> 2p <sup>5</sup> 3d <sup>2</sup> | <sup>2</sup> D <sub>3/2</sub>                  | 3d    | <sup>2</sup> D <sub>3/2</sub> | 15.194           | 15.170              | 0.48  | 0.06 | 1.7      | 1.2      | 1.9                 | 0.18          | 0.22          | 0.34      | 0.43      | *  |
| 212 | 5   | 2s <sup>2</sup> 2p <sup>5</sup> 3d <sup>2</sup> | <sup>2</sup> D <sub>3/2</sub>                  | 3d    | <sup>2</sup> D <sub>5/2</sub> | 15.205           | 15.178              | 0.18  |      | 1.2      |          | 0.7                 |               |               |           |           | *  |
| 213 | 4   | 2s <sup>2</sup> 2p <sup>5</sup> 3d <sup>2</sup> | <sup>2</sup> P <sub>3/2</sub>                  | 3d    | <sup>2</sup> D <sub>3/2</sub> | 15.168           | 15.150              | 1.9   | 0.62 | 3.6      | 2.9      | 0.76                | 3.7           | 3.0           | 4.3       | 3.5       |    |
| 213 | 5   | 2s <sup>2</sup> 2p <sup>5</sup> 3d <sup>2</sup> | <sup>2</sup> P <sub>3/2</sub>                  | 3d    | <sup>2</sup> D <sub>5/2</sub> | 15.179           | 15.158              | 3.7   |      | 3.4      | 4.1      | 1.5                 |               |               |           |           |    |
| 214 | 4   | 2s <sup>2</sup> 2p <sup>5</sup> 3d <sup>2</sup> | <sup>2</sup> P <sub>1/2</sub>                  | 3d    | <sup>2</sup> D <sub>3/2</sub> | 15.077           | 15.097              | 1.0   | 0.81 | 1.5      | 1.2      | 0.59                | 2.6           | 2.2           | 3.3       | 2.6       |    |

The first columns give the upper  $j$  and lower  $i$  level number, and the main configurations from the  $n=6$  model. For the lower  $C_i$  the 2s<sup>2</sup> 2p<sup>6</sup> is omitted. The following two columns list the theoretical wavelengths (Å) from the  $n=6$  model and from Phillips et al. (1997) (P). The following three columns list the  $F_2$  values from the present  $n=6$  model, the Phillips et al. and Cornille et al. (1994) (C) ones, in units of  $10^{13}$ . Only the strongest observable lines with  $F_2$  values larger than  $10^{13}$  are shown. The following columns show the A-values and the total AI rates from the autoionizing state, also in units of  $10^{13}$ . The AI  $n = 3$  is obtained with the  $n = 3$  set and KUTOO=1. The B98 are the AI rates calculated with Cowan's code by Bruch et al. (1998) whilst the N86 are the YODA ones from Nilsen (1989). An asterisk in the last column indicates differences in the AI rates that can affect the line intensity, as the ratio  $Y$  differs from unity, with the exception of the transitions where inner-shell (IS in the last column) is a dominant process.

from the list of the fluxes observed with the KAP crystal, assuming a simple Gaussian broadening with a FWHM=0.025 Å.

The P75 wavelengths are so accurate, down to a few mÅ, that have been used as reference wavelengths for several X-ray lines. Most of the weaker P75 lines were unidentified. Several turn out to be due to satellite lines from Fe xvii, as discussed below.

It is interesting to note that the poorly cited laboratory study by Cohen & Feldman (1970) lists several lines which are within a few mÅ of the P75 ones. The spectrum was obtained with a 3m high-resolution spectrograph, from a low-inductance iron vacuum spark. At the time most of the lines were unidentified, but the class of the line listed by Cohen & Feldman (1970) and the wavelength coincidences with the P75 suggests that several of the satellite lines discussed below were also observed in the vacuum spark.

The Solar Maximum Mission (SMM) Flat Crystal Spectrometer (FCS) also produced spectra of quiescent active regions, but with too short exposures and low signal. The instrument was always pointed at the brightest parts, where the hot core loops typically have 3-4 MK. We have searched the entire SMM FCS database

for suitable observations of the satellite lines, but encountered the following problems. First, the count rates of a single bin of each crystal scan are very low, hence to increase the signal to noise several scans need to be averaged. Second, significant variability in the strong lines is often present. In our previous analysis of FCS data (Del Zanna & Mason 2014), we focused on very stable and quiescent scans, where variability is reduced. However, the signal in the satellite lines is too low in those spectra.

We have also analysed spectra during, or after, large flares. In those cases the signal in the lines is generally higher, but that in the satellite lines is lower. Additionally, hotter lines from e.g. Fe xviii and Fe xix appear and further complicate the analysis of the spectra.

We found that the best case is a series of five scans taken on 1987-Apr-19 between 15:54 and 16:42 UT. Some variability was present, and three spectra were scaled by small amounts (10, 20, and 30%) before averaging, to compensate for the variability. The spectrum was then smoothed, converted to calibrated units, and increased by a factor of 2.7 to match approximately the reconstructed AR spectra of P75. The two spectra, plotted in Figure 2, show a re-



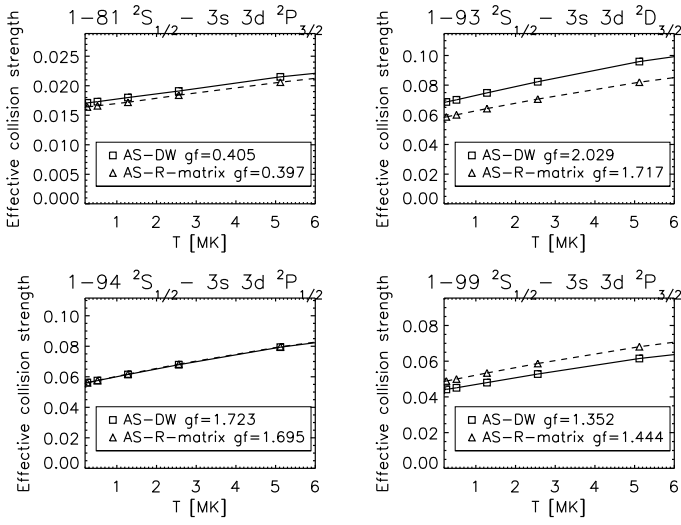


**Figure 1.** A comparison between the rate coefficients calculated with the DW approximation ( $n = 6$  model) and those with the  $R$ -matrix codes and the  $n = 3$  model calculated by Liang et al.

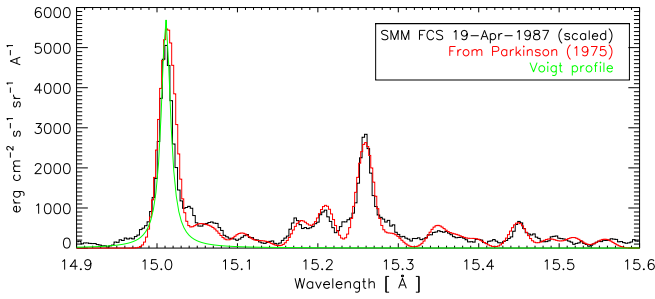


**Figure 2.** A comparison between the averaged SMM/FCS spectrum of an active region and that reconstructed from the fluxes tabulated by P75, in the spectral region where the main Fe XVII satellite lines are present. The FCS instrumental Voigt profile of the Fe XVII resonance line is shown in green.

markable similarity. The P75 spectrum was clearly of much higher quality, as even the weakest satellite lines were measurable (with about 50 total counts).

The main difference between the observed and reconstructed P75 spectra are the broad features surrounding the Fe XVII 15.01 and 15.26 Å 3C and 3D lines. The FCS instrumental line profile is well approximated with a Voigt function. We have taken the profile of the Fe XVII 16.75 Å line and fitted with a Voigt profile, which is also plotted (rescaled by the peak intensity) in Figure 2, to show that in fact there is significant signal in the wings of the resonance line at 15.01 Å, especially in the red wing, with two broad features at 15.04 and 15.07 Å, which were listed at 15.05 and 15.07 Å by P75. The main difference is that the broad feature at 15.04 Å is much stronger than the other one, in the FCS spectra. This results from the slightly better spectral resolution of the FCS instrument.

Something similar is present in the red wing of the 15.26 Å line, where P75 list a feature at 15.293 Å, although the FCS spectrum indicates a broader and brighter feature. The FCS spectrum also shows a broad feature in the blue wing of the 3D 15.26 Å line. Inspection of the spectra in Fig. 1b of P75 also indicates broadenings around the two Fe XVII lines.

We have slightly improved the previous emission measure

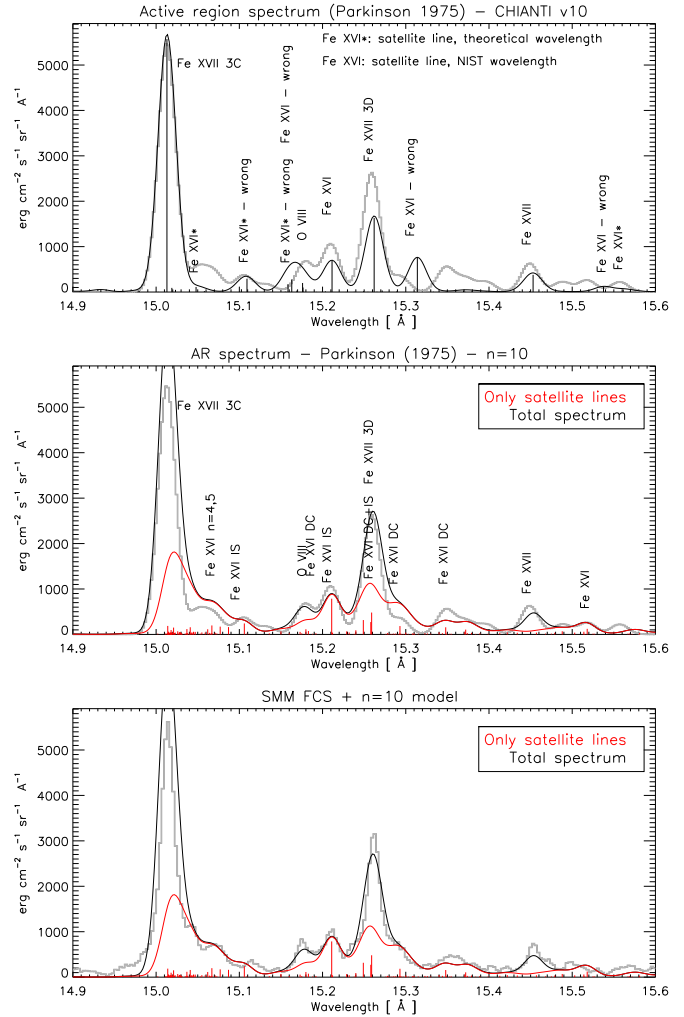


**Figure 3.** A comparison between the reconstructed P75 spectrum (grey thick line) and an averaged SMM/FCS spectrum of an active region with the CHIANTI v.10 data (top plot) and the present  $n = 10$  model in the 15-15.6 Å region. The CHIANTI (NIST) wavelengths of the main lines are incorrect, with one exception. A few satellite lines mainly formed by inner-shell (IS) excitation or dielectronic capture (DC) are indicated.

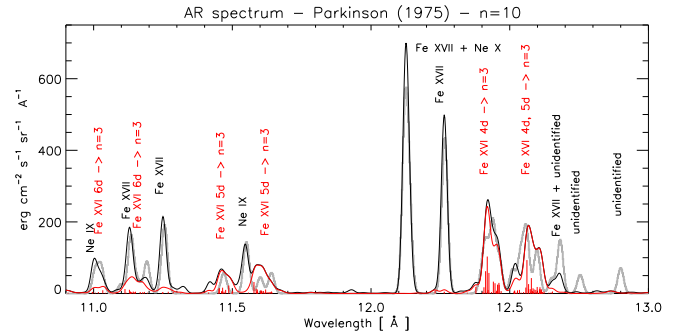


**Figure 4.** A comparison between the reconstructed P75 spectrum (grey thick line) and the present  $n = 10$  model, indicating that several previously unidentified lines are due to Fe XVI. The red spectrum is the contribution from the satellite lines.

**Table 7.** List of the strongest satellite lines from AI states of Fe XVI.

| Present | B79     | P75           | CF70    | G09    | Transition (lower-upper)                             | $I_o$ | $I_p$                | levels     |
|---------|---------|---------------|---------|--------|--|-------|----------------------|------------|
| 12.42   | -       | 12.414        | 12.411? | -      | 3s $^2S_{1/2}$ - 2s $^2$ 2p $^5$ 3s 4d $^2P_{1/2}$   | 3.4   | -,1.5,1.7,1.6,1.7    | 1-(336)380 |
| 12.42   | -       | 12.414        | 12.411? | -      | 3s $^2S_{1/2}$ - 2s $^2$ 2p $^5$ 3s 4d $^2P_{3/2}$   |       | -,1.2,?,2.7,2.8      | 1-(334)378 |
| 12.43   | -       | -             | 12.427? | -      | 3p $^2P_{3/2}$ - 2s $^2$ 2p $^5$ 3p 4d $^2D_{5/2}$   |       | -,2.4,1.6,1.5,1.5    | 3-(522)566 |
| 12.56   | -       | 12.560        | -       | -      | 3s $^2S_{1/2}$ - 2s $^2$ 2p $^5$ 3s 4d $^4D_{3/2}$   | 4.7   | -,3.0,2.7,2.5,2.5    | 1-(298)342 |
| 14.00   | -       | 14.037        | 14.020? | 14.03? | 3s $^2S_{1/2}$ - 2s 2p $^6$ 3s 3p $^2P_{3/2}$        | 4.5   | -,0.8,1.3,1.2,1.3    | 1-(193)237 |
| 15.11   | 15.163p | 15.105        | 15.110  | 15.111 | 3s $^2S_{1/2}$ - 2s $^2$ 2p $^5$ 3s 3d $^2P_{3/2}$   | 9.8   | 7.2,7.4,6.6,6.7,6.5  | 1-(99)143  |
| 15.17   | -       | ?             | 15.158? | -      | 3d $^2D_{3/2}$ - 2s $^2$ 2p $^5$ 3d $^2$ $^2P_{3/2}$ |       | -,2.2,1.7,1.6,1.5    | 4-(213)257 |
| 15.18   | -       | 15.179        | 15.173? | -      | 3d $^2D_{5/2}$ - 2s $^2$ 2p $^5$ 3d $^2$ $^2P_{3/2}$ | 18    | -,4.1,3.1,3.2,3.0    | 5-(213)257 |
| 15.18   | -       | 15.179        | -       | -      | 3p $^2P_{3/2}$ - 2s $^2$ 2p $^5$ 3p 3d $^2P_{1/2}$   |       | 3.0,2.5,2.4,2.1,2.0  | 3-(156)200 |
| 15.21   | 15.211p | 15.210        | 15.222? | 15.210 | 3s $^2S_{1/2}$ - 2s $^2$ 2p $^5$ 3s 3d $^2P_{1/2}$   | 28    | 18,20.9,21.7,21,21   | 1-(94)138  |
| 15.24   | -       | 15.259(bl 3D) | -       | -      | 3d $^2D_{5/2}$ - 2s $^2$ 2p $^5$ 3d $^2$ $^2D_{5/2}$ |       | -,3.4,2.4,2.6,2.4    | 5-(211)255 |
| 15.25   | -       | 15.259(bl 3D) | 15.237? | -      | 3d $^2D_{5/2}$ - 2s $^2$ 2p $^5$ 3d $^2$ $^2F_{7/2}$ | 70    | -,12.0,8.9,8.9,8.5   | 5-(210)254 |
| 15.26   | -       | 15.259(bl 3D) | 15.261  | -      | 3p $^2P_{1/2}$ - 2s $^2$ 2p $^5$ 3p 3d $^2D_{3/2}$   |       | 8.0,10.6,7.8,7.8,7.3 | 2-(151)195 |
| 15.26   | 15.314p | 15.259(bl 3D) | 15.261  | 15.261 | 3s $^2S_{1/2}$ - 2s $^2$ 2p $^5$ 3s 3d $^2D_{3/2}$   |       | 20,13.8,11.9,13.7,13 | 1-(93)137  |
| 15.29   | -       | 15.293(bl)    | 15.288? | -      | 3p $^2P_{3/2}$ - 2s $^2$ 2p $^5$ 3p 3d $^2D_{5/2}$   | 9.3   | 4.8,6.9,5.0,5.2,4.9  | 3-(152)196 |
| 15.35   | -       | 15.348        | 15.341  | -      | 3d $^2D_{3/2}$ - 2s $^2$ 2p $^5$ 3d $^2$ $^2F_{5/2}$ | 14    | -,3.6,2.7,4.4,4.2    | 4-(201)245 |
| 15.37   | -       | 15.348        | 15.341  | -      | 3d $^2D_{3/2}$ - 2s $^2$ 2p $^5$ 3d $^2$ $^2F_{5/2}$ |       | -,5.8,4.3,3.0,2.8    | 4-(200)244 |
| 15.49   | -       | 15.488        | 15.490? | -      | 3d $^2D_{5/2}$ - 2s $^2$ 2p $^5$ 3d $^2$ $^2G_{7/2}$ | 5.9   | -,1.9,2.4,2.0,1.9    | 5-(191)235 |
| 15.52   | 15.538p | 15.518        | -       | 15.516 | 3s $^2S_{1/2}$ - 2s $^2$ 2p $^5$ 3s 3d $^2P_{3/2}$   | 6.9   | 3.1,5.3,5.3,3.3,3.3  | 1-(81)125  |

The first column gives the present wavelengths. The following three columns indicate the possible wavelength matches from Burkhalter et al. (1979) [B79, p for predicted] and from the lists of the unidentified lines in Parkinson (1975) [P75] and Cohen & Feldman (1970) [CF70]. The next column lists the observed wavelengths from Graf et al. (2009) [G09].  $I_o$  indicates the radiance in  $\text{ergs cm}^{-2} \text{sr}^{-1} \text{s}^{-1}$  from P75, as described in Del Zanna (2011), while  $I_p$  list the predicted values (the first from the CHIANTI model, then those obtained from the  $n = 4, 5, 6, 10$  models). The last column indicates the indices of the transition, relative to the  $n = 6$  (in brackets) and  $n = 10$  models.

analyses of the P75 data described in Del Zanna (2011) and Del Zanna & Mason (2014), and calculated a predicted spectrum. We used CHIANTI v.10 (Del Zanna et al. 2021) data, except for the satellite lines. Table 7 lists a selection of the strongest lines within the P75 spectral range. We list our ab-initio AS wavelength, and the wavelengths of the lines we identify in the Parkinson (1975) and Cohen & Feldman (1970) spectra. Whenever possible, we are also listing the observed wavelengths from Graf et al. (2009). In the last columns we provide the radiances, as measured by P75 and as calculated with the various models.

Clearly, all the satellite lines are blended to some degree, so the comparisons with the spectra, shown in Figure 3, are more instructive. We have adjusted the energies of a few main states (cf. the energy table) to produce the spectra.

The top plot in Figure 3 clearly indicates that the CHIANTI (NIST) wavelengths of the main lines are incorrect, with one exception; and that, even for the active region spectra, there is significant missing flux due to the satellite lines. The new  $n = 10$  model increases the flux significantly, and brings the predicted intensity of the 3D line in to good agreement with observations.

Figure A1 in the Appendix shows the results from the  $n = 6$  model, to show the effects of the additional  $n = 7 - 10$  configurations in blending the 3C resonance line.

We have calculated the total flux of the Fe XVII and the satellite lines in the 15–15.7 Å range at 2 MK and found an increase of a factor of 1.93 with the  $n = 10$  model (a factor of 1.8 with the  $n = 6$  one), relative to the total flux of the current CHIANTI model. Indeed, at such low temperatures, the satellite lines dominate this spectral range.

We discuss below a few details about the main lines, noting that it is nearly impossible to list all previous identifications,

whether correct or incorrect. The labelling is from the  $n = 6$  model. We are relatively confident about our identifications, but ultimately new high-resolution laboratory and solar spectra will be needed to confirm the present work.

## 5.1 The 15–16 Å region

The strongest line is the decay to the ground state of the 3s3d  $^2P_{1/2}$  (level No. 94), mainly formed by inner-shell excitation. The energy of the upper state was estimated by B76 from the decay to the 3d  $^2D_{5/2}$ , observed at 16.952 Å. The AS ab-initio wavelength is very close (15.21) to the value estimated by B76 (15.211) and to the solar and lab measurements by P75 and G09 (15.210). The predicted radiance is 22, close to the observed one (28.1).

The second strongest line is the decay to the ground state of the 2s $^2$  2p $^5$  3s 3d  $^2D_{3/2}$  (level No 93), also formed by inner-shell excitation. The B76 predicted wavelength is 15.314 Å, from an energy of 6530000., obtained from the decay to the 3d  $^2D_{5/2}$  at 17.087 Å. This identification is clearly incorrect for various reasons. First, there is no solar line at 15.314 Å. Second, the predicted energy is very far from our ab-initio value. Given the predicted intensity and wavelength, this line must be blending the strong Fe xvii 3D observed by P75 at 15.259 Å. The same conclusion was obtained by G09, and earlier by Brown et al. (2001).

Our model predicts a nearby strong line (2–151). We assume it is also blended with the Fe xvii 3D line, which provides an excellent comparison between predicted and observed spectra. With this identification, we obtain an energy of 6830703  $\text{cm}^{-1}$ , close to the value of a state with the same J value and parity given by D13 at 6831282  $\text{cm}^{-1}$ . This line is not listed by G09. What seems to be the same transition (Na5) was predicted by M05 to be at a very simi-

**Table 8.** List of newly identified satellite lines, Parkinson’s KAP crystal.

| $\lambda_{\text{obs}}(\text{\AA})$ | Int | P75     | upper        |
|------------------------------------|-----|---------|--------------|
| 10.742                             | 1.3 | Ne IX   | bl $n=7,8$   |
| 11.006                             | 1.7 | Na X    | bl $n=6$     |
| 11.027                             | 2.0 | Ne IX   | bl $n=6$     |
| 11.099                             | 0.7 | Na X    | bl $n=6$     |
| 11.135                             | 4.3 | Fe XVII | bl $n=5,6$   |
| 11.160                             | 0.9 | unid.   | $n=6$        |
| 11.192                             | 2.4 | Na X    | $n=4$        |
| 11.469                             | 1.5 | unid.   | $n=5$        |
| 11.601                             | 1.2 | unid.   | $n=5,6$      |
| 11.641                             | 1.5 | unid.   | $n=5$        |
| 12.399                             | 1.2 | unid.   | $n=4$        |
| 12.414                             | 3.4 | unid.   | $n=4$        |
| 12.439                             | 5.2 | unid.   | $n=4$        |
| 12.463                             | 2.4 | unid.   | $n=4$        |
| 12.510                             | 1.8 | unid.   | $n=4,5$      |
| 12.539                             | 2.8 | unid.   | $n=4,5$      |
| 12.560                             | 4.7 | unid.   | $n=4,5$      |
| 12.598                             | 3.3 | unid.   | $n=4,5$      |
| 12.651                             | 1.1 | Ni XIX  | bl $n=4,5$   |
| 13.868                             | 2.1 | unid.   | $n=4,5$      |
| 13.899                             | 5.8 | Fe XVII | bl $n=3,4,5$ |
| 14.037                             | 4.5 | Ni XIX  | bl $n=3$     |
| 14.081                             | 3.4 | Ni XIX  | bl $n=3$     |
| 17.16                              | 8.9 | unid.   | $n=3$        |
| 17.21                              | 12. | unid.   | $n=3$        |
| 17.40                              | 7.9 | unid.   | $n=3$        |
| 17.51                              | 5.1 | unid.   | $n=3$        |
| 17.77                              | 5.4 | O VII   | bl $n=3$     |

The columns give the observed wavelengths, the radiance in  $\text{ergs cm}^{-2} \text{sr}^{-1} \text{s}^{-1}$ , P75 identification (unid. for unidentified lines) and the upper states of the main satellite lines. bl indicates blending with satellite lines.

lar wavelength, 15.255 Å, but was actually identified with a line at 15.276 Å. As there is no strong solar line at 15.276 Å, the M05 identification seems incorrect.

The third strongest line, mostly formed by inner-shell excitation, is the decay to the ground state from the  $2p^5 3s 3d^2 P_{3/2}$  (level No 99), with an AS predicted wavelength of 15.11 Å. The energy of the upper state was estimated by B76 to be 6595000 from the decay to the  $3d^2 D_{3/2}$ , observed at 16.890 Å. This predicts the decay to the ground state at 15.163 Å, which is not observed. Again, this was an incorrect identification by B76. We identify, on the basis of wavelength and intensity, with the P75 solar line at 15.105 Å, observed in the laboratory by CF70 and G09 at 15.11 Å.

There are several other cases where the B76 / NIST identifications are incorrect. One clear case, where lines are not too blended, is the decay from the  $3s 3d^2 P_{3/2}$  (level No. 81). The AS predicted wavelength is 15.54 Å. It could either be the solar line at 15.518 or that one at 15.557 Å, while B76 predicted, on an incorrect identification of the decay to the  $3d^2 D_{5/2}$ , a wavelength of 15.538 Å, where a solar line is not observed. We favour the first option, as the wavelength agrees with the Díaz et al. (2013) calculations, and its intensity is well matched. G09 has a predicted wavelength of 15.533 Å but gives an observed wavelength of 15.516 Å, despite the fact that there is no line clearly visible at that wavelength in their spectrum of Fig. 2.

Our model predicts many strong lines from the  $2p^5 3d^2$  configuration, which was not included by Liang et al. (2008). Such

states were not considered by G09, as the lines are formed by DC. Surprisingly, such states were also not considered by B76. M05 list only two transitions, from  $J = 5/2$  to  $3d^2 D_{3/2}$  (Na2b, 15.360 Å), and from  $J = 3/2$  to  $3d^2 D_{3/2}$ , at a predicted wavelength of 15.200 Å. In our model, we actually have two strong transitions from two nearby  $J = 5/2$  states to the  $3d^2 D_{3/2}$ , at predicted wavelengths of 15.34 and 15.36 Å. They are likely blended to form the strong solar line at 15.348 Å. The model spectrum agrees very well with the P75 and FCS spectra. On the other hand, transitions from  $J = 3/2$  to  $3d^2 D_{3/2}$  are relatively weak in our model.

G09 found a blue wing around 15.19 Å and identified it with the transition 3–155 in their model, with a relative intensity of 0.18. The present model instead predicts a very weak relative intensity of 0.03. On the other hand, our model predicts two strong decays from the  $2s^2 2p^5 3d^2$  (5–211 and 5–210) which are most likely blending the 15.21 and 15.26 Å lines. We obtain a good agreement between predicted and observed spectra with these identifications. One of the two lines, the 5–211, was instead identified by M05 with a line in the Hercules spectra at 15.237 Å from a predicted wavelength of 15.225, although their spectra also have a strong line at 15.213 Å. The M05 identification is inconsistent with the present model, as there is no strong solar line at 15.237 Å.

We also identify a strong transition (3–152), with predicted wavelength of 15.30 Å with the solar one observed by P75 at 15.293 Å (plus a blend of  $n=5$  lines), considering that intensities and wavelengths match. This line is not listed by G09. What seems to be the same transition (Na3) was predicted by M05 to be at a very similar wavelength, 15.290 Å, but was actually identified with a line at 15.304 Å.

## 5.2 The satellites blending the 3C line at 15 Å.

We note that the large number of transitions from  $n = 4, 5$  states provide ab-initio wavelengths and intensities in broad agreement with the FCS observation. Several transitions from  $n = 4, 5$  states are either blending the resonance line, or are scattered across many different spectral ranges.

The  $n = 4$  satellites to the 3C line are mostly resolvable, being in the red wing, but the others are not. As previously mentioned, we have carried out a large-scale  $n = 10$  calculation to improve the estimate of all the satellites of the 3C line. Most of the flux is due to transitions from  $n = 4, 5$  states, but as Beiersdorfer et al. (2011) pointed out, some contribution from higher states is also present.

If one considers only the  $2p^5 3d nl$  satellites within the 15.0–15.06 Å, which contribute about 75% of the total flux in this band with the  $n = 10$  model, the  $n = 4, 5, 6$  states contribute most, with 16, 33 and 15% respectively. The  $n = 7, 8, 9, 10$  states contribute progressively less: 9.5, 8.3, 5.3, and 3.9%. Therefore, any missing flux due to even higher states would likely be at most a few percent.

Finally, to assess the possible missing flux, we have carried out a configuration-averaged complete calculation including configurations up to  $n = 30$ . The wavelengths of the transitions are not very accurate, and if one considers decays from individual configurations some discrepancies are found with the totals from the  $j$ -resolved  $n = 10$  model, hence comparisons between the calculations are not simple. If one considers the main transitions from the  $2p^5 3d nl$  states, the  $n = 30$  model indicates that those from the  $n = 4 - 10$  states contribute 91%, those from the  $n = 11 - 20$  states 6% and those from the  $n = 21 - 30$  states 3%. However, the total flux within the 3C line from the  $n = 30$  model is less than 2% larger than what we calculated with the  $n = 10$  model. Therefore, we conclude that any missing flux within the  $n = 10$  model

would amount only to a few percent, in broad agreement with the Beiersdorfer et al. (2011) FAC result.

### 5.3 The 10–15 Å region

As shown in Figure 4, our model predicts many transitions blending known transitions or explaining previously unidentified lines. Table 8 provides a short summary. There are many transitions from  $n = 6$  states that are blending known lines from Ne IX and Fe XVII between 11.0 and 11.3 Å. Within the 11.45 and 11.50 Å and 11.60 and 11.65 Å regions, our model predicts several decays from  $2s^2 2p^5 3l 5d$  states. Parkinson's spectrum has indeed unidentified transitions at 11.469, 11.601, and 11.641 with intensities similar to the predicted ones.

Within the 12.3 and 12.7 Å region, there are several relatively strong transitions from  $2s^2 2p^5 3l 4l'$  and some  $n = 5$  states. Parkinson's spectrum has many unidentified transitions in this wavelength range. There is an excellent match between our ab-initio wavelengths and calculated intensities and the observed spectrum.

Several decays from  $1s^2 2s 2p^6 3p 5f$  and  $5g$  states are predicted between 13.8 and 13.9 Å and are blending the Fe XVII 13.899 Å line, which is significantly under-predicted, and form the unidentified line at 13.868 Å.

Several transitions of the type  $1s^2 2s 2p^6 3l 3l''$  are predicted around 14.0 Å, are blending Ni XIX lines around 14.04 Å.

### 5.4 The 17–18 Å region

The situation for the weaker lines above 17 Å is rather unclear, as the calculations are more uncertain, and the sensitivity of the solar instruments was lower, hence only a few of the stronger lines were observed. G09 list various identifications for lines formed by inner-shell excitation, but agreement with the observed spectrum is poor. P75 only lists four unidentified lines, at 17.151, 17.199, 17.389 (blended with O VII), and 17.501 Å. However, all the lines in Parkinson's spectrum above 16 Å have an incorrect wavelength, being lower by 0.01 Å. We have applied such correction to the spectra, see Table 8.

G09 lists several possible lines in the 17.37–17.42 Å range, a few others at 17.447 Å, and several others in the range 17.494–17.510 Å, i.e. effectively the laboratory spectrum has the same lines as the solar one (including a blend of emission for the first two lines). Our model also predicts many lines mostly formed by DC, but none that stand out for their brightness, so identifications are very difficult.

The brightest is a decay from  $3s 3p^4 D_{7/2}$  (level No.38) to the  $3p^2 P_{3/2}$ , predicted at 17.63 Å. G09 has a similar predicted wavelength (17.619 Å), but gives an observed wavelength of 17.592 Å, which does not agree with the solar spectrum. D13 does not provide a calculated energy for the upper state, nor B76.

Similarly, there are several lines from low-lying states that our model predicts around 17.55 Å. The strongest of them, the decay of the  $3s 3d^4 P_{5/2}$  to the  $3d^2 D_{5/2}$ , has a wavelength predicted by Liang et al. (2008) of 17.36 Å, but was instead identified by B76 with a line at 17.498 Å. Our identification agrees with G09.

## 6 CONCLUSIONS

Despite being a century from their discovery, satellite lines are still relatively poorly known. The literature on the identifications of the

strongest lines is very confusing. Proper modelling requires large-scale calculations of accurate atomic data and further studies. From our brief summary of previous studies, both theoretical and experimental, it is clear that, especially for the satellite lines of Na-like iron, further studies are needed to benchmark the atomic data and to obtain experimental wavelengths. It is also clear that different theoretical approaches can provide significantly different models.

Such work is particularly important for Fe XVI as the satellite lines can be relatively strong and blend the Fe XVII 3C and 3D lines, which are among the most important X-ray lines, because of their plasma diagnostic use. We found that the missing flux around the 3C and 3D lines, about a factor of 2 as found from the analysis of the first MaGIXS flight, is mostly due to decays from autoionizing states of Fe XVI.

We have also identified for the first time many other lines in the X-rays, and showed that some are also blending previously known lines. It is clear that a complete knowledge of these satellite lines is important when analysing astrophysical observations at these wavelengths, for example from the recently launched XRISM satellite. It is also clear that further calculations for other ions are needed.

Our comparison to the best available solar high-resolution spectra is very satisfactory, but further observations are needed to test the models. In this respect, the current NASA proposals for further sounding rockets with an improved MaGIXS instrument are very important.

## ACKNOWLEDGMENTS

GDZ acknowledges support from STFC (UK) via the consolidated grants to the atomic astrophysics group (AAG) at DAMTP, University of Cambridge (ST/P000665/1. and ST/T000481/1). The UK APAP network is funded by STFC via the consolidated grant (PI Badnell) to the University of Strathclyde (ST/V000683/1).

## DATA AVAILABILITY

The results of the largest, fine-structure resolved calculation are made available at ZENODO in CHIANTI ascii format, for easy inclusion.

## REFERENCES

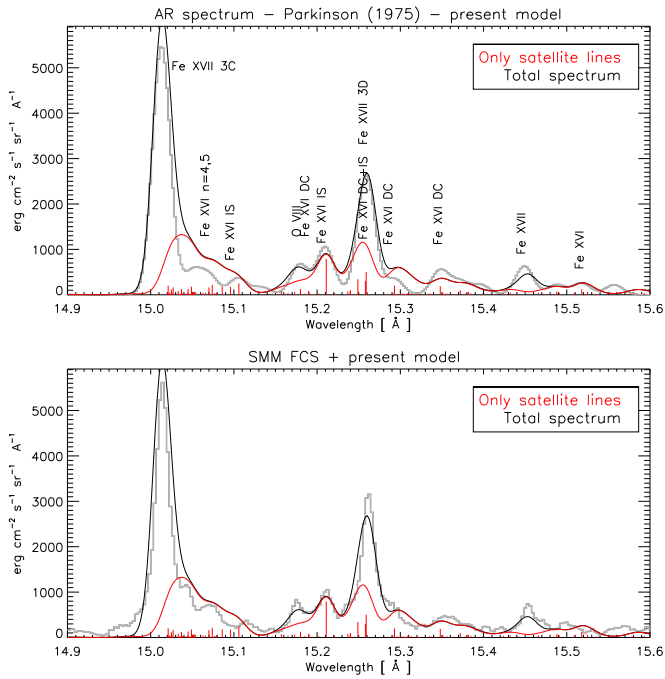
- Aggarwal K. M., Keenan F. P., 2007, *A&A*, 463, 399
- Badnell N. R., 2011, *Computer Physics Communications*, 182, 1528
- Beiersdorfer P., Bode M. P., Ishikawa Y., Diaz F., 2014, *ApJ*, 793, 99
- Beiersdorfer P., Diaz F., Ishikawa Y., 2012, *ApJ*, 745, 167
- Beiersdorfer P., Gu M. F., Lepson J., Desai P., 2011, in *Johns-Krull C., Browning M. K., West A. A., eds, 16th Cambridge Workshop on Cool Stars, Stellar Systems, and the Sun Vol. 448 of Astronomical Society of the Pacific Conference Series, A New Temperature Determination Using the Fe XVII Emission of Capella*. p. 787
- Beiersdorfer P., Hell N., Lepson J. K., 2018, *ApJ*, 864, 24
- Berrington K. A., Eissner W. B., Norington P. H., 1995, *Computer Physics Communications*, 92, 290
- Brown G. V., Beiersdorfer P., Chen H., Chen M. H., Reed K. J., 2001, *ApJ*, 557, L75



- Bruch R., Safronova U. I., Shlyaptseva A. S., Nilsen J., Schneider D., 1998, *J. Quant. Spec. Radiat. Transf.*, 60, 605
- Burkhalter P. G., Cohen L., Cowan R. D., Feldman U., 1979, *Journal of the Optical Society of America (1917-1983)*, 69, 1133
- Cohen L., Feldman U., 1970, *ApJ*, 160, L105
- Cornille M., Dubau J., Faucher P., Bely-Dubau F., Blancard C., 1994, *A&AS*, 105, 77
- Del Zanna G., 2011, *A&A*, 536, A59
- Del Zanna G., Dere K. P., Young P. R., Landi E., 2021, *ApJ*, 909, 38
- Del Zanna G., Mason H. E., 2014, *A&A*, 565, A14
- Del Zanna G., Mason H. E., 2018, *Living Reviews in Solar Physics*, 15, 5
- Dere K. P., Del Zanna G., Young P. R., Landi E., Sutherland R. S., 2019, *ApJS*, 241, 22
- Díaz F., Vilkas M. J., Ishikawa Y., Beiersdorfer P., 2013, *ApJS*, 207, 11
- Dubau J., Volonte S., 1980, *Reports on Progress in Physics*, 43, 199
- Gabriel A. H., 1972, *MNRAS*, 160, 99
- Gabriel A. H., Paget T. M., 1972, *Journal of Physics B Atomic Molecular Physics*, 5, 673
- Graf A., Beiersdorfer P., Brown G. V., Gu M. F., 2009, *ApJ*, 695, 818
- Hummer D. G., Berrington K. A., Eissner W., Pradhan A. K., Saraph H. E., Tully J. A., 1993, *A&A*, 279, 298
- Jupen C., Engstrom L., Hutton R., Trabert E., 1988, *Journal of Physics B Atomic Molecular Physics*, 21, L347
- Kramida A., Yu. Ralchenko Reader J., and NIST ASD Team, 2022, *NIST Atomic Spectra Database (ver. 5.10)*, [Online]. Available: <https://physics.nist.gov/asd> [2023, June 26]. National Institute of Standards and Technology, Gaithersburg, MD.
- Kühn S., Cheung C., Oreshkina N. S., Steinbrügge R., Togawa M., Bernitt S., Berger L., Buck J., Hoesch M., Seltmann J., Trinter F., Keitel C. H., Kozlov M. G., Porsev S. G., Gu M. F., Porter F. S., Pfeifer T., Leutenegger M. A., Harman Z., Safronova M. S., López-Urrutia J. R. C., Shah C., 2022, *Phys. Rev. Lett.*, 129, 245001
- Liang G. Y., Badnell N. R., 2010, *A&A*, 518, A64+
- Liang Y., Whiteford A. D., Badnell N. R., 2008, *Journal of Physics B Atomic Molecular Physics*, 41, 235203
- Loch S. D., Pindzola M. S., Ballance C. P., Griffin D. C., 2006, *Journal of Physics B Atomic Molecular Physics*, 39, 85
- May M. J., Beiersdorfer P., Dunn J., Jordan N., Hansen S. B., Osterheld A. L., Faenov A. Y., Pikuz T. A., Skobelev I. Y., Flora F., Bollanti S., Di Lazzaro P., Murra D., Reale A., Reale L., Tomasetti G., Ritucci A., Francucci M., Martellucci S., Petrocelli G., 2005, *ApJS*, 158, 230
- Nilsen J., 1989, *Atomic Data and Nuclear Data Tables*, 41, 131
- Parkinson J. H., 1975, *Sol. Phys.*, 42, 183
- Phillips K. J. H., Greer C. J., Bhatia A. K., Coffey I. H., Barnsley R., Keenan F. P., 1997, *A&A*, 324, 381
- Quigley L., Berrington K., 1996, *Journal of Physics B Atomic Molecular Physics*, 29, 4529
- Quigley L., Berrington K., Pelan J., 1998, *Computer Physics Communications*, 114, 225
- Safronova U. I., Johnson W. R., Safronova M. S., Albritton J. R., 2002, *Phys. Rev. A*, 66, 052511
- Savage S. L., Winebarger A. R., Kobayashi K., Athiray P. S., Beabout D., Golub L., Walsh R. W., Beabout B., Bradshaw S., Bruccoleri A. R., Champey P. R., Cheimets P., Cirtain J., DeLuca E. E., Del Zanna G., Dudík J., Guillory A., Haight H., Heilmann R. K., Hertz E., Hogue W., Kegley J., Kolodziejczak J., Madsen C., Mason H., McKenzie D. E., Ranganathan J., Reeves K. K., Robertson B., Schattensburg M. L., Scholvin J., Siler R., Testa P., Vigil G. D., Warren H. P., Watkinson B., Weddendorf B., Wright E., 2023, *ApJ*, 945, 105
- Shirai T., Sugar J., Musgrove A., Wiese W., 2000, *Spectral Data for Highly Ionized Atoms: Ti, V, Cr, Mn, Fe, Co, Ni, Cu, Kr, and Mo. Vol. 8 of J. Phys. Chem. Ref. Data, Monograph*, American Institute of Physics, Melville, NY

**Table A1.** The target electron configuration basis and orbital scaling parameters  $\lambda_{nl}$  for the structure run of Liang et al.

| Configurations                                |    |         |    |         |
|---|----|---------|----|---------|
| $1s^2 2s^2 2p^6 3l$ ( $l=s,p,d$ )             | 1s | 1.39364 |    |         |
| $1s^2 2s^2 2p^5 3l 3l'$ ( $l=s,p,d, l'=s,p$ ) | 2s | 1.08686 | 3s | 1.15588 |
|   | 2p | 1.02341 | 3p | 1.11371 |
|   | 3d | 1.15100 |    |         |

**Figure A1.** A comparison between the reconstructed P75 spectrum (grey thick line) and an averaged SMM/FCS spectrum of an active region with the present  $n = 6$  model in the 15-15.6 Å region.**APPENDIX A: ADDITIONAL MATERIAL****Table A2.** List of the main states.

| $i$ | Conf.             | P | T           | $E_{\text{exp}}$   | $E_{\text{AS}}$ | $E_{\text{Diaz+}}$ | $E_{\text{Liang+}}$ |
|-----|-------------------|---|-------------|--------------------|-----------------|--------------------|---------------------|
| 1   | $2s^2 2p^6 3s$    | e | $^2S_{1/2}$ | 0                  | 0               | 0                  | 0                   |
| 2   | $2s^2 2p^6 3p$    | o | $^2P_{1/2}$ | 277194             | 276293          | 277222             | 276436              |
| 3   | $2s^2 2p^6 3p$    | o | $^2P_{3/2}$ | 298143             | 298373          | 298167             | 296534              |
| 4   | $2s^2 2p^6 3d$    | e | $^2D_{3/2}$ | 675501             | 674642          | 675463             | 676373              |
| 5   | $2s^2 2p^6 3d$    | e | $^2D_{5/2}$ | 678405             | 679275          | 678372             | 679712              |
| 77  | $2s^2 2p^5 3s^2$  | o | $^2P_{3/2}$ | 5773000?           | 5748000         | 5756556            | 5802584             |
| 78  | $2s^2 2p^5 3s^2$  | o | $^2P_{1/2}$ | 5873000?           | 5850943         | 5857665            | 5899697             |
| 79  | $2s^2 2p^5 3s 3p$ | e | $^4S_{3/2}$ | -                  | 5941810         | 5953391            | 5991935             |
| 80  | $2s^2 2p^5 3s 3p$ | e | $^4D_{5/2}$ | 5982000            | 5970059         | 5980479            | 6020272             |
| 81  | $2s^2 2p^5 3s 3p$ | e | $^4D_{7/2}$ | -                  | 5976391         | 5986775            | 6026148             |
| 82  | $2s^2 2p^5 3s 3p$ | e | $^2P_{3/2}$ | -                  | 5977178         | 5987047            | 6027021             |
| 83  | $2s^2 2p^5 3s 3p$ | e | $^2P_{1/2}$ | 6001000            | 5989400         | 5999543            | 6041011             |
| 84  | $2s^2 2p^5 3s 3p$ | e | $^4P_{5/2}$ | 6013000            | 6001435         | 6011855            | 6053544             |
| 85  | $2s^2 2p^5 3s 3p$ | e | $^2D_{3/2}$ | 6013000            | 6002818         | 6012375            | 6053898             |
| 86  | $2s^2 2p^5 3s 3p$ | e | $^2S_{1/2}$ | 6042000?           | 6019309         | 6027754            | 6076536             |
| 87  | $2s^2 2p^5 3s 3p$ | e | $^4D_{1/2}$ | 6075000            | 6068977         | 6077192            | 6113566             |
| 88  | $2s^2 2p^5 3s 3p$ | e | $^4P_{1/2}$ | 6089000?           | 6074866         | 6082835            | 6128206             |
| 89  | $2s^2 2p^5 3s 3p$ | e | $^4D_{3/2}$ | 6089000            | 6079784         | 6087509            | 6124285             |
| 90  | $2s^2 2p^5 3s 3p$ | e | $^2D_{5/2}$ | -                  | 6090463         | 6096282            | 6141431             |
| 91  | $2s^2 2p^5 3s 3p$ | e | $^4P_{3/2}$ | 6096000            | 6091914         | 6100268            | 6138528             |
| 92  | $2s^2 2p^5 3s 3p$ | e | $^2D_{5/2}$ | 6110000            | 6101305         | 6108077            | 6147237             |
| 93  | $2s^2 2p^5 3s 3p$ | e | $^2P_{3/2}$ | 6129000            | 6108503         | 6113831            | 6157761             |
| 94  | $2s^2 2p^5 3s 3p$ | e | $^2P_{1/2}$ | -                  | 6181158         | 6182346            | 6229457             |
| 95  | $2s^2 2p^5 3s 3p$ | e | $^2D_{3/2}$ | 6217000?           | 6198457         | 6201702            | 6244142             |
| 96  | $2s^2 2p^5 3s 3p$ | e | $^2S_{1/2}$ | 6267000?           | 6253611         | 6245187            | 6313279             |
| 111 | $2s^2 2p^5 3s 3d$ | o | $^4P_{5/2}$ | 6393000            | 6382976         | 6390567            | 6440048             |
| 112 | $2s^2 2p^5 3s 3d$ | o | $^4F_{9/2}$ | -                  | 6383060         | 6389221            | 6438162             |
| 117 | $2s^2 2p^5 3s 3d$ | o | $^4F_{5/2}$ | 6406000            | 6397726         | 6404701            | 6453145             |
| 118 | $2s^2 2p^5 3p^2$  | o | $^2P_{3/2}$ | -                  | 6400493         | 6406003            | 6469670             |
| 119 | $2s^2 2p^5 3s 3d$ | o | $^2D_{3/2}$ | 6419000            | 6408540         | 6415660            | 6464402             |
| 120 | $2s^2 2p^5 3p^2$  | o | $^2D_{3/2}$ | -                  | 6415643         | 6422064            | 6455698             |
| 121 | $2s^2 2p^5 3s 3d$ | o | $^4D_{7/2}$ | 6422000            | 6416259         | 6421329            | 6471649             |
| 122 | $2s^2 2p^5 3p^2$  | o | $^2D_{5/2}$ | -                  | 6418038         | 6423498            | 6464730             |
| 123 | $2s^2 2p^5 3s 3d$ | o | $^2P_{1/2}$ | 6423000            | 6418066         | 6423578            | 6476262             |
| 124 | $2s^2 2p^5 3s 3d$ | o | $^2F_{5/2}$ | 6425000            | 6420114         | 6425339            | 6474699             |
| 125 | $2s^2 2p^5 3s 3d$ | o | $^2P_{3/2}$ | <del>6436000</del> | 6439623         | 6443091            | 6498398             |
|     |                   |   |             | <b>6444100?</b>    |                 |                    |                     |
| 126 | $2s^2 2p^5 3s 3d$ | o | $^4D_{1/2}$ | -                  | 6450153         | 6455202            | 6506414             |
| 127 | $2s^2 2p^5 3s 3d$ | o | $^4D_{3/2}$ | <del>6473000</del> | 6479009         | 6483365            | 6536053             |
| 128 | $2s^2 2p^5 3s 3d$ | o | $^2F_{7/2}$ | <del>6445000</del> | 6483824         | 6485011            | 6546990             |
| 129 | $2s^2 2p^5 3s 3d$ | o | $^4F_{3/2}$ | 6502000            | 6496562         | 6502061            | 6547383             |
| 130 | $2s^2 2p^5 3s 3d$ | o | $^2D_{5/2}$ | <del>6464000</del> | 6498874         | 6501608            | 6555370             |
| 131 | $2s^2 2p^5 3s 3d$ | o | $^4D_{5/2}$ | 6502000            | 6499710         | 6504077            | 6549706             |

$E_{\text{exp}}$  gives the NIST experimental energies, except the those in bold which are our tentative values.  $E_{\text{AS}}$  are our ab-initio AS energies with the  $n = 10$  model.  $E_{\text{Diaz+}}$  are the energies from Díaz et al. (2013) while  $E_{\text{Liang+}}$  are the AS ones from Liang et al. (2008).

Table A2. Contd

| $i$ | Conf.             | P | T           | $E_{\text{NIST}}$                     | $E_{\text{AS}}$ | $E_{\text{Diaz+}}$ | $E_{\text{Liang+}}$ |
|-----|-------------------|---|-------------|---------------------------------------|-----------------|--------------------|---------------------|
| 132 | $2s^2 2p^5 3p^2$  | o | $^2P_{1/2}$ | -                                     | 6507356         | 6508883            | 6566725             |
| 133 | $2s^2 2p^5 3s 3d$ | o | $^2D_{5/2}$ | 6516000                               | 6511948         | 6514575            | 6569938             |
| 134 | $2s^2 2p^5 3s 3d$ | o | $^2F_{7/2}$ | 6517000                               | 6512092         | 6514871            | 6561652             |
| 135 | $2s^2 2p^5 3p^2$  | o | $^2P_{1/2}$ | -                                     | 6512966         | 6514341            | 6579688             |
| 136 | $2s^2 2p^5 3p^2$  | o | $^2P_{3/2}$ | -                                     | 6530425         | 6531608            | 6592253             |
| 137 | $2s^2 2p^5 3s 3d$ | o | $^2D_{3/2}$ | <del>6530000</del><br><b>6553500?</b> | 6551020         | 6550184            | 6611638             |
| 138 | $2s^2 2p^5 3s 3d$ | o | $^2P_{1/2}$ | 6574000                               | 6576810         | 6573657            | 6644694             |
| 139 | $2s^2 2p^5 3p 3d$ | e | $^4D_{1/2}$ | -                                     | 6589929         | 6601400            | 6646599             |
| 140 | $2s^2 2p^5 3s 3d$ | o | $^2F_{5/2}$ | <del>6556000</del>                    | 6594116         | 6593543            | 6651977             |
| 141 | $2s^2 2p^5 3p 3d$ | e | $^4D_{3/2}$ | -                                     | 6598110         | 6608991            | 6654887             |
| 142 | $2s^2 2p^5 3p 3d$ | e | $^4D_{5/2}$ | -                                     | 6610901         | 6620899            | 6667902             |
| 143 | $2s^2 2p^5 3s 3d$ | o | $^2P_{3/2}$ | <del>6595000</del><br><b>6620000?</b> | 6619300         | 6616740            | 6686516             |
| 195 | $2s^2 2p^5 3p 3d$ | e | $^2D_{3/2}$ | <b>6831000?</b>                       | 6834145         | 6831282            | 6894915             |
| 196 | $2s^2 2p^5 3p 3d$ | e | $^2D_{5/2}$ | <b>6837100?</b>                       | 6839169         | 6838045            | 6893483             |
| 235 | $2s^2 2p^5 3d^2$  | o | $^2G_{7/2}$ | <b>7135000?</b>                       | 7132714         | 7134361            | -                   |
| 236 | $2s^2 2p^5 3d^2$  | o | $^4F_{5/2}$ | -                                     | 7139463         | 7142053            | -                   |
| 237 | $2s 2p^6 3s 3p$   | o | $^2P_{3/2}$ | -                                     | 7140998         | 7128949            | -                   |
| 244 | $2s^2 2p^5 3d^2$  | o | $^2F_{5/2}$ | <b>7180800?</b>                       | 7185725         | 7186088            | -                   |
| 245 | $2s^2 2p^5 3d^2$  | o | $^2F_{5/2}$ | <b>7191000?</b>                       | 7190776         | 7193832            | -                   |
| 254 | $2s^2 2p^5 3d^2$  | o | $^2F_{7/2}$ | <b>7236000?</b>                       | 7243251         | 7242818            | -                   |
| 255 | $2s^2 2p^5 3d^2$  | o | $^2D_{5/2}$ | <b>7240000?</b>                       | 7252103         | 7246119            | -                   |
| 256 | $2s^2 2p^5 3d^2$  | o | $^2D_{3/2}$ | -                                     | 7258926         | 7253388            | -                   |
| 257 | $2s^2 2p^5 3d^2$  | o | $^2P_{3/2}$ | <b>7266000?</b>                       | 7270449         | 7263947            | -                   |

Table A3: Energies

| $i$ | Conf.             | P | T            | $E_{\text{NIST}}$ | $E_{\text{AS}}$ | $E_{\text{Diaz+}}$ | $E_{\text{Liang+}}$ |
|-----|-------------------|---|--------------|-------------------|-----------------|--------------------|---------------------|
| 1   | $2s^2 2p^6 3s$    | e | $^2S_{1/2}$  | 0                 | 0               | 0                  | 0                   |
| 2   | $2s^2 2p^6 3p$    | o | $^2P_{1/2}$  | 277194            | 277711          | 277222             | 276436              |
| 3   | $2s^2 2p^6 3p$    | o | $^2P_{3/2}$  | 298143            | 300089          | 298167             | 296534              |
| 4   | $2s^2 2p^6 3d$    | e | $^2D_{3/2}$  | 675501            | 676579          | 675463             | 676373              |
| 5   | $2s^2 2p^6 3d$    | e | $^2D_{5/2}$  | 678405            | 681330          | 678372             | 679712              |
| 6   | $2s^2 2p^6 4s$    | e | $^2S_{1/2}$  | 1867740           | 1869087         | 1867664            | 1867895             |
| 7   | $2s^2 2p^6 4p$    | o | $^2P_{1/2}$  | 1977649           | 1979132         | 1977616            | 1977070             |
| 8   | $2s^2 2p^6 4p$    | o | $^2P_{3/2}$  | 1985649           | 1987870         | 1985786            | 1984703             |
| 9   | $2s^2 2p^6 4d$    | e | $^2D_{3/2}$  | 2124719           | 2126589         | 2124584            | 2124092             |
| 10  | $2s^2 2p^6 4d$    | e | $^2D_{5/2}$  | 2125959           | 2128787         | 2125923            | 2125524             |
| 11  | $2s^2 2p^6 4f$    | o | $^2F_{5/2}$  | 2184960           | 2184613         | 2184910            | 2184919             |
| 12  | $2s^2 2p^6 4f$    | o | $^2F_{7/2}$  | 2185409           | 2185387         | 2185401            | 2185424             |
| 13  | $2s^2 2p^6 5s$    | e | $^2S_{1/2}$  | 2662000           | 2663585         | 2663328            | 2662751             |
| 14  | $2s^2 2p^6 5p$    | o | $^2P_{1/2}$  | 2717169           | 2717783         | 2717620            | 2716785             |
| 15  | $2s^2 2p^6 5p$    | o | $^2P_{3/2}$  | 2721159           | 2722230         | 2721636            | 2720472             |
| 16  | $2s^2 2p^6 5d$    | e | $^2D_{3/2}$  | 2788049           | 2789109         | 2788713            | 2787715             |
| 17  | $2s^2 2p^6 5d$    | e | $^2D_{5/2}$  | 2788609           | 2790271         | 2789416            | 2788448             |
| 18  | $2s^2 2p^6 5f$    | o | $^2F_{5/2}$  | 2818599           | 2818306         | 2818974            | 2818342             |
| 19  | $2s^2 2p^6 5f$    | o | $^2F_{7/2}$  | 2818900           | 2818714         | 2819226            | 2818601             |
| 20  | $2s^2 2p^6 5g$    | e | $^2G_{7/2}$  | 2822700           | 2821171         | 0                  | 2821317             |
| 21  | $2s^2 2p^6 5g$    | e | $^2G_{9/2}$  | 2822800           | 2821402         | 0                  | 2821470             |
| 22  | $2s^2 2p^6 6s$    | e | $^2S_{1/2}$  | 3075999           | 3075690         | 0                  | 3075119             |
| 23  | $2s^2 2p^6 6p$    | o | $^2P_{1/2}$  | 3106400           | 3106229         | 0                  | 3105599             |
| 24  | $2s^2 2p^6 6p$    | o | $^2P_{3/2}$  | 3108899           | 3108902         | -                  | 3107635             |
| 25  | $2s^2 2p^6 6d$    | e | $^2D_{3/2}$  | 3146070           | 3146303         | -                  | 3145288             |
| 26  | $2s^2 2p^6 6d$    | e | $^2D_{5/2}$  | 3146670           | 3147021         | -                  | 3145709             |
| 27  | $2s^2 2p^6 6f$    | o | $^2F_{5/2}$  | 3163129           | 3162874         | -                  | 3162816             |
| 28  | $2s^2 2p^6 6f$    | o | $^2F_{7/2}$  | 3163190           | 3163122         | -                  | 3162966             |
| 29  | $2s^2 2p^6 6g$    | e | $^2G_{7/2}$  | -                 | 3164672         | -                  | 3164757             |
| 30  | $2s^2 2p^6 6g$    | e | $^2G_{9/2}$  | -                 | 3164807         | -                  | 3164846             |
| 31  | $2s^2 2p^6 6h$    | o | $^2H_{9/2}$  | -                 | 3164858         | -                  | 3164916             |
| 32  | $2s^2 2p^6 6h$    | o | $^2H_{11/2}$ | -                 | 3164947         | -                  | 3164976             |
| 33  | $2s^2 2p^5 3s^2$  | o | $^2P_{3/2}$  | 5773000?          | 5744641         | 5756556            | 5802584             |
| 34  | $2s^2 2p^5 3s^2$  | o | $^2P_{1/2}$  | 5873000?          | 5848114         | 5857665            | 5899697             |
| 35  | $2s^2 2p^5 3s 3p$ | e | $^4S_{3/2}$  | -                 | 5939043         | 5953391            | 5991935             |
| 36  | $2s^2 2p^5 3s 3p$ | e | $^4D_{5/2}$  | 5982000           | 5967095         | 5980479            | 6020272             |
| 37  | $2s^2 2p^5 3s 3p$ | e | $^4D_{7/2}$  | -                 | 5973428         | 5986775            | 6026148             |
| 38  | $2s^2 2p^5 3s 3p$ | e | $^2P_{3/2}$  | -                 | 5974184         | 5987047            | 6027021             |
| 39  | $2s^2 2p^5 3s 3p$ | e | $^2P_{1/2}$  | 6001000           | 5986456         | 5999543            | 6041011             |
| 40  | $2s^2 2p^5 3s 3p$ | e | $^4P_{5/2}$  | 6013000           | 5998400         | 6011855            | 6053544             |
| 41  | $2s^2 2p^5 3s 3p$ | e | $^2D_{3/2}$  | 6013000           | 5999767         | 6012375            | 6053898             |
| 42  | $2s^2 2p^5 3s 3p$ | e | $^2S_{1/2}$  | 6042000?          | 6016544         | 6027754            | 6076536             |
| 43  | $2s^2 2p^5 3s 3p$ | e | $^4D_{1/2}$  | 6075000           | 6066510         | 6077192            | 6113566             |
| 44  | $2s^2 2p^5 3s 3p$ | e | $^4P_{1/2}$  | 6089000?          | 6072233         | 6082835            | 6128206             |
| 45  | $2s^2 2p^5 3s 3p$ | e | $^4D_{3/2}$  | 6089000           | 6077288         | 6087509            | 6124285             |
| 46  | $2s^2 2p^5 3s 3p$ | e | $^2D_{5/2}$  | -                 | 6087412         | 6096282            | 6141431             |
| 47  | $2s^2 2p^5 3s 3p$ | e | $^4P_{3/2}$  | 6096000           | 6089389         | 6100268            | 6138528             |
| 48  | $2s^2 2p^5 3s 3p$ | e | $^2D_{5/2}$  | 6110000           | 6098693         | 6108077            | 6147237             |
| 49  | $2s^2 2p^5 3s 3p$ | e | $^2P_{3/2}$  | 6129000?          | 6105380         | 6113831            | 6157761             |
| 50  | $2s^2 2p^5 3s 3p$ | e | $^2P_{1/2}$  | -                 | 6178837         | 6182346            | 6229457             |
| 51  | $2s^2 2p^5 3s 3p$ | e | $^2D_{3/2}$  | 6217000?          | 6195854         | 6201702            | 6244142             |
| 52  | $2s^2 2p^5 3s 3p$ | e | $^2S_{1/2}$  | 6267000?          | 6252510         | 6245187            | 6313279             |
| 53  | $2s^2 2p^5 3p^2$  | o | $^4P_{3/2}$  | -                 | 6257463         | 6269659            | 6316508             |
| 54  | $2s^2 2p^5 3p^2$  | o | $^2P_{1/2}$  | -                 | 6258792         | 6271517            | 6317822             |
| 55  | $2s^2 2p^5 3p^2$  | o | $^4P_{5/2}$  | -                 | 6265662         | 6278181            | 6324087             |
| 56  | $2s^2 2p^5 3p^2$  | o | $^2F_{7/2}$  | -                 | 6276200         | 6287623            | 6328785             |
| 57  | $2s^2 2p^5 3p^2$  | o | $^2P_{3/2}$  | -                 | 6278747         | 6291100            | 6334949             |
| 58  | $2s^2 2p^5 3p^2$  | o | $^4P_{1/2}$  | -                 | 6295965         | 6307896            | 6353532             |
| 59  | $2s^2 2p^5 3p^2$  | o | $^2D_{5/2}$  | -                 | 6297314         | 6308932            | 6350782             |
| 60  | $2s^2 2p^5 3p^2$  | o | $^2D_{3/2}$  | -                 | 6298455         | 6308901            | 6352715             |
| 61  | $2s^2 2p^5 3p^2$  | o | $^4D_{7/2}$  | -                 | 6303014         | 6314133            | 6356554             |
| 62  | $2s^2 2p^5 3p^2$  | o | $^4D_{5/2}$  | -                 | 6304417         | 6315498            | 6358568             |
| 63  | $2s^2 2p^5 3p^2$  | o | $^4D_{1/2}$  | -                 | 6353354         | 6362006            | 6404267             |
| 64  | $2s^2 2p^5 3s 3d$ | o | $^4P_{1/2}$  | -                 | 6356616         | 6369713            | 6418318             |



Table A3: (continued)

| <i>i</i> | Conf.   | P | T                              | $E_{\text{NIST}}$                     | $E_{\text{AS}}$ | $E_{\text{Diaz+}}$ | $E_{\text{Liang+}}$ |
|----------|---|---|--------------------------------|---------------------------------------|-----------------|--------------------|---------------------|
| 65       | 2s <sup>2</sup> 2p <sup>5</sup> 3p <sup>2</sup> | o | <sup>4</sup> S <sub>3/2</sub>  | -                                     | 6357933         | 6368079            | 6411844             |
| 66       | 2s <sup>2</sup> 2p <sup>5</sup> 3s 3d           | o | <sup>4</sup> P <sub>3/2</sub>  | -                                     | 6365097         | 6377262            | 6426196             |
| 67       | 2s <sup>2</sup> 2p <sup>5</sup> 3s 3d           | o | <sup>4</sup> P <sub>5/2</sub>  | 6393000                               | 6379612         | 6390567            | 6440048             |
| 68       | 2s <sup>2</sup> 2p <sup>5</sup> 3s 3d           | o | <sup>4</sup> F <sub>9/2</sub>  | -                                     | 6379790         | 6389221            | 6438162             |
| 69       | 2s <sup>2</sup> 2p <sup>5</sup> 3p <sup>2</sup> | o | <sup>4</sup> D <sub>3/2</sub>  | -                                     | 6381562         | 6390640            | 6432092             |
| 70       | 2s <sup>2</sup> 2p <sup>5</sup> 3p <sup>2</sup> | o | <sup>2</sup> F <sub>5/2</sub>  | -                                     | 6385341         | 6394058            | 6431790             |
| 71       | 2s <sup>2</sup> 2p <sup>5</sup> 3s 3d           | o | <sup>4</sup> F <sub>7/2</sub>  | -                                     | 6385866         | 6396084            | 6444453             |
| 72       | 2s <sup>2</sup> 2p <sup>5</sup> 3p <sup>2</sup> | o | <sup>2</sup> S <sub>1/2</sub>  | -                                     | 6390585         | 6398771            | 6439224             |
| 73       | 2s <sup>2</sup> 2p <sup>5</sup> 3s 3d           | o | <sup>4</sup> F <sub>5/2</sub>  | 6406000                               | 6394429         | 6404701            | 6453145             |
| 74       | 2s <sup>2</sup> 2p <sup>5</sup> 3p <sup>2</sup> | o | <sup>2</sup> P <sub>3/2</sub>  | -                                     | 6397961         | 6406003            | 6469670             |
| 75       | 2s <sup>2</sup> 2p <sup>5</sup> 3s 3d           | o | <sup>2</sup> D <sub>3/2</sub>  | 6419000                               | 6405385         | 6415660            | 6464402             |
| 76       | 2s <sup>2</sup> 2p <sup>5</sup> 3p <sup>2</sup> | o | <sup>2</sup> D <sub>3/2</sub>  | -                                     | 6413008         | 6422064            | 6455698             |
| 77       | 2s <sup>2</sup> 2p <sup>5</sup> 3s 3d           | o | <sup>4</sup> D <sub>7/2</sub>  | 6422000                               | 6413123         | 6421329            | 6471649             |
| 78       | 2s <sup>2</sup> 2p <sup>5</sup> 3s 3d           | o | <sup>2</sup> P <sub>1/2</sub>  | -                                     | 6415027         | 6423498            | 6464730             |
| 79       | 2s <sup>2</sup> 2p <sup>5</sup> 3s 3d           | o | <sup>2</sup> F <sub>5/2</sub>  | 6423000                               | 6415181         | 6423578            | 6476262             |
| 80       | 2s <sup>2</sup> 2p <sup>5</sup> 3p <sup>2</sup> | o | <sup>2</sup> D <sub>5/2</sub>  | 6425000                               | 6417371         | 6425339            | 6474699             |
| 81       | 2s <sup>2</sup> 2p <sup>5</sup> 3s 3d           | o | <sup>2</sup> P <sub>3/2</sub>  | <del>6426000</del><br><b>6444100?</b> | 6436676         | 6443091            | 6498398             |
| 82       | 2s <sup>2</sup> 2p <sup>5</sup> 3s 3d           | o | <sup>4</sup> D <sub>1/2</sub>  | -                                     | 6447867         | 6455202            | 6506414             |
| 83       | 2s <sup>2</sup> 2p <sup>5</sup> 3s 3d           | o | <sup>4</sup> D <sub>3/2</sub>  | <del>6473000</del>                    | 6476481         | 6483365            | 6536053             |
| 84       | 2s <sup>2</sup> 2p <sup>5</sup> 3s 3d           | o | <sup>2</sup> F <sub>7/2</sub>  | <del>6445000</del>                    | 6480673         | 6485011            | 6546990             |
| 85       | 2s <sup>2</sup> 2p <sup>5</sup> 3s 3d           | o | <sup>4</sup> F <sub>3/2</sub>  | 6502000                               | 6493786         | 6502061            | 6547383             |
| 86       | 2s <sup>2</sup> 2p <sup>5</sup> 3s 3d           | o | <sup>2</sup> D <sub>5/2</sub>  | <del>6464000</del>                    | 6495941         | 6501608            | 6549706             |
| 87       | 2s <sup>2</sup> 2p <sup>5</sup> 3s 3d           | o | <sup>4</sup> D <sub>5/2</sub>  | 6502000                               | 6496993         | 6504077            | 6555370             |
| 88       | 2s <sup>2</sup> 2p <sup>5</sup> 3p <sup>2</sup> | o | <sup>2</sup> P <sub>1/2</sub>  | -                                     | 6504938         | 6508883            | 6566725             |
| 89       | 2s <sup>2</sup> 2p <sup>5</sup> 3s 3d           | o | <sup>2</sup> D <sub>5/2</sub>  | 6516000                               | 6508973         | 6514575            | 6569938             |
| 90       | 2s <sup>2</sup> 2p <sup>5</sup> 3s 3d           | o | <sup>2</sup> F <sub>7/2</sub>  | 6517000                               | 6509407         | 6514871            | 6561652             |
| 91       | 2s <sup>2</sup> 2p <sup>5</sup> 3p <sup>2</sup> | o | <sup>2</sup> P <sub>1/2</sub>  | -                                     | 6511585         | 6514341            | 6579688             |
| 92       | 2s <sup>2</sup> 2p <sup>5</sup> 3p <sup>2</sup> | o | <sup>2</sup> P <sub>3/2</sub>  | -                                     | 6528784         | 6531608            | 6592253             |
| 93       | 2s <sup>2</sup> 2p <sup>5</sup> 3s 3d           | o | <sup>2</sup> D <sub>3/2</sub>  | <del>6530000</del><br><b>6553500?</b> | 6549199         | 6550184            | 6611638             |
| 94       | 2s <sup>2</sup> 2p <sup>5</sup> 3s 3d           | o | <sup>2</sup> P <sub>1/2</sub>  | 6574000                               | 6575409         | 6573657            | 6644694             |
| 95       | 2s <sup>2</sup> 2p <sup>5</sup> 3p 3d           | e | <sup>4</sup> D <sub>1/2</sub>  | -                                     | 6586884         | 6601400            | 6646599             |
| 96       | 2s <sup>2</sup> 2p <sup>5</sup> 3s 3d           | o | <sup>2</sup> F <sub>5/2</sub>  | <del>6556000</del>                    | 6591507         | 6593543            | 6651977             |
| 97       | 2s <sup>2</sup> 2p <sup>5</sup> 3p 3d           | e | <sup>4</sup> D <sub>3/2</sub>  | -                                     | 6595119         | 6608991            | 6654887             |
| 98       | 2s <sup>2</sup> 2p <sup>5</sup> 3p 3d           | e | <sup>4</sup> D <sub>5/2</sub>  | -                                     | 6607993         | 6620899            | 6667902             |
| 99       | 2s <sup>2</sup> 2p <sup>5</sup> 3s 3d           | o | <sup>2</sup> P <sub>3/2</sub>  | <del>6595000</del><br><b>6620000?</b> | 6617260         | 6616740            | 6686516             |
| 100      | 2s <sup>2</sup> 2p <sup>5</sup> 3p 3d           | e | <sup>4</sup> D <sub>7/2</sub>  | -                                     | 6623086         | 6634662            | 6682013             |
| 101      | 2s <sup>2</sup> 2p <sup>5</sup> 3p 3d           | e | <sup>4</sup> G <sub>7/2</sub>  | -                                     | 6629973         | 6640658            | 6685459             |
| 102      | 2s <sup>2</sup> 2p <sup>5</sup> 3p 3d           | e | <sup>4</sup> G <sub>9/2</sub>  | -                                     | 6631373         | 6641641            | 6685281             |
| 103      | 2s <sup>2</sup> 2p <sup>5</sup> 3p 3d           | e | <sup>2</sup> D <sub>5/2</sub>  | -                                     | 6634688         | 6645828            | 6692155             |
| 104      | 2s <sup>2</sup> 2p <sup>5</sup> 3p 3d           | e | <sup>4</sup> G <sub>11/2</sub> | -                                     | 6636164         | 6646042            | 6690008             |
| 105      | 2s <sup>2</sup> 2p <sup>5</sup> 3p 3d           | e | <sup>2</sup> D <sub>3/2</sub>  | -                                     | 6639303         | 6650162            | 6696538             |
| 106      | 2s <sup>2</sup> 2p <sup>5</sup> 3p 3d           | e | <sup>4</sup> G <sub>5/2</sub>  | -                                     | 6649416         | 6659988            | 6704606             |
| 107      | 2s <sup>2</sup> 2p <sup>5</sup> 3p 3d           | e | <sup>2</sup> F <sub>7/2</sub>  | -                                     | 6650899         | 6660419            | 6704344             |
| 108      | 2s <sup>2</sup> 2p <sup>5</sup> 3p 3d           | e | <sup>2</sup> P <sub>1/2</sub>  | -                                     | 6652928         | 6664075            | 6708793             |
| 109      | 2s <sup>2</sup> 2p <sup>5</sup> 3p 3d           | e | <sup>4</sup> P <sub>1/2</sub>  | -                                     | 6661688         | 6673499            | 6721372             |
| 110      | 2s <sup>2</sup> 2p <sup>5</sup> 3p 3d           | e | <sup>2</sup> G <sub>7/2</sub>  | -                                     | 6663503         | 6673065            | 6718402             |
| 111      | 2s <sup>2</sup> 2p <sup>5</sup> 3p 3d           | e | <sup>4</sup> P <sub>3/2</sub>  | -                                     | 6666392         | 6678388            | 6725771             |
| 112      | 2s <sup>2</sup> 2p <sup>5</sup> 3p 3d           | e | <sup>4</sup> F <sub>9/2</sub>  | -                                     | 6675064         | 6684395            | 6729992             |
| 113      | 2s <sup>2</sup> 2p <sup>5</sup> 3p 3d           | e | <sup>4</sup> P <sub>5/2</sub>  | -                                     | 6676103         | 6686826            | 6736070             |
| 114      | 2s <sup>2</sup> 2p <sup>5</sup> 3p 3d           | e | <sup>4</sup> S <sub>3/2</sub>  | -                                     | 6676694         | 6686155            | 6731171             |
| 115      | 2s <sup>2</sup> 2p <sup>5</sup> 3p 3d           | e | <sup>4</sup> D <sub>7/2</sub>  | -                                     | 6678774         | 6688328            | 6733893             |
| 116      | 2s <sup>2</sup> 2p <sup>5</sup> 3p 3d           | e | <sup>4</sup> D <sub>5/2</sub>  | -                                     | 6679065         | 6689006            | 6735168             |
| 117      | 2s <sup>2</sup> 2p <sup>5</sup> 3p 3d           | e | <sup>4</sup> P <sub>3/2</sub>  | -                                     | 6686282         | 6696202            | 6742881             |
| 118      | 2s <sup>2</sup> 2p <sup>5</sup> 3p 3d           | e | <sup>4</sup> F <sub>3/2</sub>  | -                                     | 6692732         | 6701502            | 6747267             |
| 119      | 2s <sup>2</sup> 2p <sup>5</sup> 3p 3d           | e | <sup>4</sup> F <sub>9/2</sub>  | -                                     | 6693560         | 6701731            | 6747879             |
| 120      | 2s <sup>2</sup> 2p <sup>5</sup> 3p 3d           | e | <sup>4</sup> D <sub>5/2</sub>  | -                                     | 6701323         | 6708959            | 6755032             |
| 121      | 2s <sup>2</sup> 2p <sup>5</sup> 3p 3d           | e | <sup>4</sup> F <sub>7/2</sub>  | -                                     | 6701728         | 6710310            | 6756669             |
| 122      | 2s <sup>2</sup> 2p <sup>5</sup> 3p 3d           | e | <sup>2</sup> F <sub>5/2</sub>  | -                                     | 6703862         | 6712468            | 6759091             |
| 123      | 2s <sup>2</sup> 2p <sup>5</sup> 3p 3d           | e | <sup>2</sup> P <sub>1/2</sub>  | -                                     | 6706716         | 6716454            | 6762890             |
| 124      | 2s <sup>2</sup> 2p <sup>5</sup> 3p 3d           | e | <sup>4</sup> D <sub>7/2</sub>  | -                                     | 6708705         | 6716199            | 6762469             |
| 125      | 2s <sup>2</sup> 2p <sup>5</sup> 3p 3d           | e | <sup>2</sup> D <sub>3/2</sub>  | -                                     | 6716985         | 6725873            | 6772014             |

Table A3: (continued)

| $i$ | Conf.   | P | T                              | $E_{\text{NIST}}$ | $E_{\text{AS}}$ | $E_{\text{Diaz+}}$ | $E_{\text{Liang+}}$ |
|-----|---|---|--------------------------------|-------------------|-----------------|--------------------|---------------------|
| 126 | 2s <sup>2</sup> 2p <sup>5</sup> 3p 3d           | e | <sup>4</sup> F <sub>5/2</sub>  | -                 | 6719573         | 6727671            | 6774524             |
| 127 | 2s <sup>2</sup> 2p <sup>5</sup> 3p 3d           | e | <sup>2</sup> D <sub>3/2</sub>  | -                 | 6721823         | 6729273            | 6779084             |
| 128 | 2s <sup>2</sup> 2p <sup>5</sup> 3p 3d           | e | <sup>2</sup> F <sub>5/2</sub>  | -                 | 6727098         | 6735550            | 6776322             |
| 129 | 2s <sup>2</sup> 2p <sup>5</sup> 3p 3d           | e | <sup>4</sup> D <sub>1/2</sub>  | -                 | 6735806         | 6741753            | 6791670             |
| 130 | 2s <sup>2</sup> 2p <sup>5</sup> 3p 3d           | e | <sup>2</sup> F <sub>5/2</sub>  | -                 | 6736348         | 6743324            | 6789725             |
| 131 | 2s <sup>2</sup> 2p <sup>5</sup> 3p 3d           | e | <sup>2</sup> S <sub>1/2</sub>  | -                 | 6741107         | 6748420            | 6798866             |
| 132 | 2s <sup>2</sup> 2p <sup>5</sup> 3p 3d           | e | <sup>2</sup> D <sub>3/2</sub>  | -                 | 6741255         | 6749251            | 6794915             |
| 133 | 2s <sup>2</sup> 2p <sup>5</sup> 3p 3d           | e | <sup>4</sup> F <sub>7/2</sub>  | -                 | 6748758         | 6756215            | 6796906             |
| 134 | 2s <sup>2</sup> 2p <sup>5</sup> 3p 3d           | e | <sup>2</sup> F <sub>5/2</sub>  | -                 | 6753395         | 6760746            | 6802029             |
| 135 | 2s <sup>2</sup> 2p <sup>5</sup> 3p 3d           | e | <sup>2</sup> F <sub>7/2</sub>  | -                 | 6762854         | 6770538            | 6812665             |
| 136 | 2s <sup>2</sup> 2p <sup>5</sup> 3p 3d           | e | <sup>2</sup> G <sub>9/2</sub>  | -                 | 6765819         | 6771871            | 6818324             |
| 137 | 2s <sup>2</sup> 2p <sup>5</sup> 3p 3d           | e | <sup>4</sup> D <sub>3/2</sub>  | -                 | 6765828         | 6771678            | 6815497             |
| 138 | 2s <sup>2</sup> 2p <sup>5</sup> 3p 3d           | e | <sup>2</sup> G <sub>9/2</sub>  | -                 | 6768948         | 6772828            | 6826856             |
| 139 | 2s <sup>2</sup> 2p <sup>5</sup> 3p 3d           | e | <sup>4</sup> F <sub>3/2</sub>  | -                 | 6774024         | 6780566            | 6827080             |
| 140 | 2s <sup>2</sup> 2p <sup>5</sup> 3p 3d           | e | <sup>4</sup> P <sub>5/2</sub>  | -                 | 6780018         | 6784892            | 6837175             |
| 141 | 2s <sup>2</sup> 2p <sup>5</sup> 3p 3d           | e | <sup>4</sup> P <sub>1/2</sub>  | -                 | 6789682         | 6795392            | 6847309             |
| 142 | 2s <sup>2</sup> 2p <sup>5</sup> 3p 3d           | e | <sup>2</sup> F <sub>7/2</sub>  | -                 | 6790910         | 6794465            | 6849062             |
| 143 | 2s <sup>2</sup> 2p <sup>5</sup> 3p 3d           | e | <sup>2</sup> D <sub>5/2</sub>  | -                 | 6794015         | 6799158            | 6844589             |
| 144 | 2s <sup>2</sup> 2p <sup>5</sup> 3p 3d           | e | <sup>2</sup> D <sub>5/2</sub>  | -                 | 6799905         | 6804620            | 6854237             |
| 145 | 2s <sup>2</sup> 2p <sup>5</sup> 3p 3d           | e | <sup>2</sup> P <sub>3/2</sub>  | -                 | 6800872         | 6806274            | 6850264             |
| 146 | 2s <sup>2</sup> 2p <sup>5</sup> 3p 3d           | e | <sup>4</sup> D <sub>3/2</sub>  | -                 | 6805430         | 6812168            | 6855813             |
| 147 | 2s <sup>2</sup> 2p <sup>5</sup> 3p 3d           | e | <sup>4</sup> D <sub>1/2</sub>  | -                 | 6805751         | 6813392            | 6855558             |
| 148 | 2s <sup>2</sup> 2p <sup>5</sup> 3p 3d           | e | <sup>2</sup> F <sub>7/2</sub>  | -                 | 6809574         | 6812846            | 6865703             |
| 149 | 2s <sup>2</sup> 2p <sup>5</sup> 3p 3d           | e | <sup>2</sup> P <sub>3/2</sub>  | -                 | 6809716         | 6814230            | 6858541             |
| 150 | 2s <sup>2</sup> 2p <sup>5</sup> 3p 3d           | e | <sup>4</sup> F <sub>5/2</sub>  | -                 | 6811249         | 6815936            | 6861713             |
| 151 | 2s <sup>2</sup> 2p <sup>5</sup> 3p 3d           | e | <sup>2</sup> D <sub>3/2</sub>  | <b>6831000?</b>   | 6833056         | 6831282            | 6894915             |
| 152 | 2s <sup>2</sup> 2p <sup>5</sup> 3p 3d           | e | <sup>2</sup> D <sub>5/2</sub>  | <b>6837100?</b>   | 6837436         | 6838045            | 6893483             |
| 153 | 2s <sup>2</sup> 2p <sup>5</sup> 3p 3d           | e | <sup>2</sup> P <sub>1/2</sub>  | -                 | 6840857         | 6841603            | 6897847             |
| 154 | 2s <sup>2</sup> 2p <sup>5</sup> 3p 3d           | e | <sup>2</sup> P <sub>3/2</sub>  | -                 | 6859775         | 6859383            | 6918774             |
| 155 | 2s 2p <sup>6</sup> 3s <sup>2</sup>              | e | <sup>2</sup> S <sub>1/2</sub>  | -                 | 6869901         | 6861675            | -                   |
| 156 | 2s <sup>2</sup> 2p <sup>5</sup> 3p 3d           | e | <sup>2</sup> P <sub>1/2</sub>  | -                 | 6883420         | 6878831            | 6941928             |
| 157 | 2s <sup>2</sup> 2p <sup>5</sup> 3p 3d           | e | <sup>2</sup> G <sub>7/2</sub>  | -                 | 6883442         | 6884423            | 6936104             |
| 158 | 2s <sup>2</sup> 2p <sup>5</sup> 3p 3d           | e | <sup>2</sup> D <sub>5/2</sub>  | -                 | 6894168         | 6888882            | 6952863             |
| 159 | 2s <sup>2</sup> 2p <sup>5</sup> 3p 3d           | e | <sup>2</sup> P <sub>3/2</sub>  | -                 | 6897773         | 6894592            | 6954817             |
| 160 | 2s <sup>2</sup> 2p <sup>5</sup> 3p 3d           | e | <sup>2</sup> S <sub>1/2</sub>  | -                 | 6915372         | 6913088            | 6972752             |
| 161 | 2s <sup>2</sup> 2p <sup>5</sup> 3p 3d           | e | <sup>2</sup> D <sub>3/2</sub>  | -                 | 6928727         | 6920217            | 6995240             |
| 162 | 2s <sup>2</sup> 2p <sup>5</sup> 3p 3d           | e | <sup>2</sup> D <sub>5/2</sub>  | -                 | 6935337         | 6926090            | 7004293             |
| 163 | 2s <sup>2</sup> 2p <sup>5</sup> 3d <sup>2</sup> | o | <sup>4</sup> D <sub>1/2</sub>  | -                 | 7025231         | 7037203            | -                   |
| 164 | 2s <sup>2</sup> 2p <sup>5</sup> 3d <sup>2</sup> | o | <sup>4</sup> D <sub>3/2</sub>  | -                 | 7028016         | 7039419            | -                   |
| 165 | 2s <sup>2</sup> 2p <sup>5</sup> 3d <sup>2</sup> | o | <sup>4</sup> D <sub>5/2</sub>  | -                 | 7032672         | 7043009            | -                   |
| 166 | 2s <sup>2</sup> 2p <sup>5</sup> 3d <sup>2</sup> | o | <sup>4</sup> D <sub>7/2</sub>  | -                 | 7040652         | 7049523            | -                   |
| 167 | 2s <sup>2</sup> 2p <sup>5</sup> 3d <sup>2</sup> | o | <sup>4</sup> G <sub>11/2</sub> | -                 | 7048994         | 7055594            | -                   |
| 168 | 2s <sup>2</sup> 2p <sup>5</sup> 3d <sup>2</sup> | o | <sup>4</sup> G <sub>9/2</sub>  | -                 | 7050157         | 7058175            | -                   |
| 169 | 2s <sup>2</sup> 2p <sup>5</sup> 3d <sup>2</sup> | o | <sup>4</sup> G <sub>7/2</sub>  | -                 | 7055533         | 7064132            | -                   |
| 170 | 2s <sup>2</sup> 2p <sup>5</sup> 3d <sup>2</sup> | o | <sup>2</sup> F <sub>5/2</sub>  | -                 | 7055676         | 7064629            | -                   |
| 171 | 2s 2p <sup>6</sup> 3s 3p                        | o | <sup>4</sup> P <sub>1/2</sub>  | -                 | 7064005         | 7058900            | -                   |
| 172 | 2s <sup>2</sup> 2p <sup>5</sup> 3d <sup>2</sup> | o | <sup>4</sup> P <sub>5/2</sub>  | -                 | 7066685         | 7074576            | -                   |
| 173 | 2s <sup>2</sup> 2p <sup>5</sup> 3d <sup>2</sup> | o | <sup>4</sup> F <sub>9/2</sub>  | -                 | 7067562         | 7073220            | -                   |
| 174 | 2s <sup>2</sup> 2p <sup>5</sup> 3d <sup>2</sup> | o | <sup>2</sup> G <sub>7/2</sub>  | -                 | 7068720         | 7075094            | -                   |
| 175 | 2s <sup>2</sup> 2p <sup>5</sup> 3d <sup>2</sup> | o | <sup>2</sup> D <sub>3/2</sub>  | -                 | 7069932         | 7078209            | -                   |
| 176 | 2s 2p <sup>6</sup> 3s 3p                        | o | <sup>4</sup> P <sub>3/2</sub>  | -                 | 7070546         | 7065086            | -                   |
| 177 | 2s <sup>2</sup> 2p <sup>5</sup> 3d <sup>2</sup> | o | <sup>2</sup> D <sub>5/2</sub>  | -                 | 7076759         | 7081804            | -                   |
| 178 | 2s <sup>2</sup> 2p <sup>5</sup> 3d <sup>2</sup> | o | <sup>4</sup> P <sub>3/2</sub>  | -                 | 7078608         | 7086971            | -                   |
| 179 | 2s 2p <sup>6</sup> 3s 3p                        | o | <sup>4</sup> P <sub>5/2</sub>  | -                 | 7083684         | 7078148            | -                   |
| 180 | 2s <sup>2</sup> 2p <sup>5</sup> 3d <sup>2</sup> | o | <sup>2</sup> P <sub>1/2</sub>  | -                 | 7086134         | 7092704            | -                   |
| 181 | 2s <sup>2</sup> 2p <sup>5</sup> 3d <sup>2</sup> | o | <sup>2</sup> H <sub>11/2</sub> | -                 | 7087677         | 7091469            | -                   |
| 182 | 2s <sup>2</sup> 2p <sup>5</sup> 3d <sup>2</sup> | o | <sup>2</sup> F <sub>7/2</sub>  | -                 | 7094562         | 7099854            | -                   |
| 183 | 2s <sup>2</sup> 2p <sup>5</sup> 3d <sup>2</sup> | o | <sup>4</sup> D <sub>5/2</sub>  | -                 | 7094609         | 7101485            | -                   |
| 184 | 2s <sup>2</sup> 2p <sup>5</sup> 3d <sup>2</sup> | o | <sup>4</sup> F <sub>3/2</sub>  | -                 | 7097492         | 7103859            | -                   |
| 185 | 2s <sup>2</sup> 2p <sup>5</sup> 3d <sup>2</sup> | o | <sup>4</sup> D <sub>7/2</sub>  | -                 | 7098186         | 7104169            | -                   |
| 186 | 2s <sup>2</sup> 2p <sup>5</sup> 3d <sup>2</sup> | o | <sup>4</sup> P <sub>1/2</sub>  | -                 | 7099272         | 7104271            | -                   |
| 187 | 2s <sup>2</sup> 2p <sup>5</sup> 3d <sup>2</sup> | o | <sup>2</sup> G <sub>9/2</sub>  | -                 | 7114444         | 7118468            | -                   |
| 188 | 2s <sup>2</sup> 2p <sup>5</sup> 3d <sup>2</sup> | o | <sup>4</sup> G <sub>5/2</sub>  | -                 | 7117849         | 7124454            | -                   |
| 189 | 2s <sup>2</sup> 2p <sup>5</sup> 3d <sup>2</sup> | o | <sup>2</sup> D <sub>3/2</sub>  | -                 | 7124454         | 7128734            | -                   |

Table A3: (continued)

| $i$ | Conf.   | P | T                             | $E_{\text{NIST}}$ | $E_{\text{AS}}$ | $E_{\text{Diaz+}}$ | $E_{\text{Liang+}}$ |
|-----|---|---|-------------------------------|-------------------|-----------------|--------------------|---------------------|
| 190 | 2s 2p <sup>6</sup> 3s 3p                        | o | <sup>2</sup> P <sub>1/2</sub> | -                 | 7127309         | 7116914            | -                   |
| 191 | 2s <sup>2</sup> 2p <sup>5</sup> 3d <sup>2</sup> | o | <sup>2</sup> G <sub>7/2</sub> | <b>7135000?</b>   | 7130233         | 7134361            | -                   |
| 192 | 2s <sup>2</sup> 2p <sup>5</sup> 3d <sup>2</sup> | o | <sup>4</sup> F <sub>5/2</sub> | -                 | 7136863         | 7142053            | -                   |
| 193 | 2s 2p <sup>6</sup> 3s 3p                        | o | <sup>2</sup> P <sub>3/2</sub> | -                 | 7138849         | 7128949            | -                   |
| 194 | 2s <sup>2</sup> 2p <sup>5</sup> 3d <sup>2</sup> | o | <sup>4</sup> S <sub>3/2</sub> | -                 | 7145140         | 7148076            | -                   |
| 195 | 2s <sup>2</sup> 2p <sup>5</sup> 3d <sup>2</sup> | o | <sup>4</sup> F <sub>7/2</sub> | -                 | 7159683         | 7163088            | -                   |
| 196 | 2s <sup>2</sup> 2p <sup>5</sup> 3d <sup>2</sup> | o | <sup>4</sup> D <sub>1/2</sub> | -                 | 7160005         | 7165078            | -                   |
| 197 | 2s <sup>2</sup> 2p <sup>5</sup> 3d <sup>2</sup> | o | <sup>2</sup> G <sub>9/2</sub> | -                 | 7169545         | 7172806            | -                   |
| 198 | 2s <sup>2</sup> 2p <sup>5</sup> 3d <sup>2</sup> | o | <sup>2</sup> P <sub>3/2</sub> | -                 | 7181008         | 7183471            | -                   |
| 199 | 2s <sup>2</sup> 2p <sup>5</sup> 3d <sup>2</sup> | o | <sup>2</sup> F <sub>7/2</sub> | -                 | 7182632         | 7185214            | -                   |
| 200 | 2s <sup>2</sup> 2p <sup>5</sup> 3d <sup>2</sup> | o | <sup>2</sup> F <sub>5/2</sub> | <b>7180800?</b>   | 7183602         | 7186088            | -                   |
| 201 | 2s <sup>2</sup> 2p <sup>5</sup> 3d <sup>2</sup> | o | <sup>2</sup> F <sub>5/2</sub> | <b>7191000?</b>   | 7188617         | 7193832            | -                   |
| 202 | 2s <sup>2</sup> 2p <sup>5</sup> 3d <sup>2</sup> | o | <sup>2</sup> S <sub>1/2</sub> | -                 | 7200182         | 7199268            | -                   |
| 203 | 2s <sup>2</sup> 2p <sup>5</sup> 3d <sup>2</sup> | o | <sup>4</sup> D <sub>3/2</sub> | -                 | 7200476         | 7203616            | -                   |
| 204 | 2s <sup>2</sup> 2p <sup>5</sup> 3d <sup>2</sup> | o | <sup>2</sup> H <sub>9/2</sub> | -                 | 7207565         | 7209123            | -                   |
| 205 | 2s <sup>2</sup> 2p <sup>5</sup> 3d <sup>2</sup> | o | <sup>2</sup> D <sub>5/2</sub> | -                 | 7210871         | 7211689            | -                   |
| 206 | 2s 2p <sup>6</sup> 3s 3p                        | o | <sup>2</sup> P <sub>1/2</sub> | -                 | 7212169         | 7199268            | -                   |
| 207 | 2s <sup>2</sup> 2p <sup>5</sup> 3d <sup>2</sup> | o | <sup>2</sup> P <sub>3/2</sub> | -                 | 7214311         | 7211685            | -                   |
| 208 | 2s 2p <sup>6</sup> 3s 3p                        | o | <sup>2</sup> P <sub>3/2</sub> | -                 | 7216411         | 7203904            | -                   |
| 209 | 2s <sup>2</sup> 2p <sup>5</sup> 3d <sup>2</sup> | o | <sup>2</sup> P <sub>1/2</sub> | -                 | 7238076         | 7235908            | -                   |
| 210 | 2s <sup>2</sup> 2p <sup>5</sup> 3d <sup>2</sup> | o | <sup>2</sup> F <sub>7/2</sub> | <b>7236000?</b>   | 7241831         | 7242818            | -                   |
| 211 | 2s <sup>2</sup> 2p <sup>5</sup> 3d <sup>2</sup> | o | <sup>2</sup> D <sub>5/2</sub> | <b>7240000?</b>   | 7251131         | 7246119            | -                   |
| 212 | 2s <sup>2</sup> 2p <sup>5</sup> 3d <sup>2</sup> | o | <sup>2</sup> D <sub>3/2</sub> | -                 | 7257952         | 7253388            | -                   |
| 213 | 2s <sup>2</sup> 2p <sup>5</sup> 3d <sup>2</sup> | o | <sup>2</sup> P <sub>3/2</sub> | <b>7266000?</b>   | 7269242         | 7263947            | -                   |
| 214 | 2s <sup>2</sup> 2p <sup>5</sup> 3d <sup>2</sup> | o | <sup>2</sup> P <sub>1/2</sub> | -                 | 7309222         | 7303627            | -                   |
| 215 | 2s 2p <sup>6</sup> 3p <sup>2</sup>              | e | <sup>4</sup> P <sub>1/2</sub> | -                 | 7384058         | 7374540            | -                   |
| 216 | 2s 2p <sup>6</sup> 3p <sup>2</sup>              | e | <sup>2</sup> D <sub>5/2</sub> | -                 | 7389574         | 7381183            | -                   |
| 217 | 2s 2p <sup>6</sup> 3p <sup>2</sup>              | e | <sup>2</sup> D <sub>3/2</sub> | -                 | 7390566         | 7382311            | -                   |
| 218 | 2s 2p <sup>6</sup> 3p <sup>2</sup>              | e | <sup>4</sup> P <sub>3/2</sub> | -                 | 7395633         | 7386567            | -                   |
| 219 | 2s 2p <sup>6</sup> 3p <sup>2</sup>              | e | <sup>4</sup> P <sub>5/2</sub> | -                 | 7411114         | 7401807            | -                   |
| 220 | 2s 2p <sup>6</sup> 3p <sup>2</sup>              | e | <sup>2</sup> P <sub>1/2</sub> | -                 | 7418366         | 7408049            | -                   |
| 221 | 2s 2p <sup>6</sup> 3p <sup>2</sup>              | e | <sup>2</sup> P <sub>3/2</sub> | -                 | 7435885         | 7425663            | -                   |
| 222 | 2s 2p <sup>6</sup> 3s 3d                        | e | <sup>4</sup> D <sub>1/2</sub> | -                 | 7480669         | 7473130            | -                   |
| 223 | 2s 2p <sup>6</sup> 3s 3d                        | e | <sup>4</sup> D <sub>3/2</sub> | -                 | 7481725         | 7473674            | -                   |
| 224 | 2s 2p <sup>6</sup> 3s 3d                        | e | <sup>4</sup> D <sub>5/2</sub> | -                 | 7483510         | 7474659            | -                   |
| 225 | 2s 2p <sup>6</sup> 3s 3d                        | e | <sup>4</sup> D <sub>7/2</sub> | -                 | 7486075         | 7476203            | -                   |
| 226 | 2s 2p <sup>6</sup> 3p <sup>2</sup>              | e | <sup>2</sup> S <sub>1/2</sub> | -                 | 7506071         | 7491289            | -                   |
| 227 | 2s 2p <sup>6</sup> 3s 3d                        | e | <sup>2</sup> D <sub>3/2</sub> | -                 | 7552884         | 7537978            | -                   |
| 228 | 2s 2p <sup>6</sup> 3s 3d                        | e | <sup>2</sup> D <sub>5/2</sub> | -                 | 7556269         | 7540221            | -                   |
| 229 | 2s 2p <sup>6</sup> 3s 3d                        | e | <sup>2</sup> D <sub>3/2</sub> | -                 | 7600455         | 7583866            | -                   |
| 230 | 2s 2p <sup>6</sup> 3s 3d                        | e | <sup>2</sup> D <sub>5/2</sub> | -                 | 7600984         | 7583934            | -                   |
| 231 | 2s <sup>2</sup> 2p <sup>5</sup> 3s 4s           | o | <sup>4</sup> P <sub>5/2</sub> | -                 | 7655895         | 7668872            | -                   |
| 232 | 2s <sup>2</sup> 2p <sup>5</sup> 3s 4s           | o | <sup>4</sup> P <sub>3/2</sub> | -                 | 7667243         | 7679557            | -                   |
| 233 | 2s <sup>2</sup> 2p <sup>5</sup> 3s 4s           | o | <sup>2</sup> P <sub>1/2</sub> | -                 | 7677217         | 7689062            | -                   |
| 234 | 2s <sup>2</sup> 2p <sup>5</sup> 3s 4s           | o | <sup>2</sup> P <sub>3/2</sub> | -                 | 7691383         | 7701732            | -                   |
| 235 | 2s 2p <sup>6</sup> 3p 3d                        | o | <sup>4</sup> F <sub>3/2</sub> | -                 | 7716155         | 7709523            | -                   |
| 236 | 2s 2p <sup>6</sup> 3p 3d                        | o | <sup>4</sup> F <sub>5/2</sub> | -                 | 7721250         | 7713928            | -                   |
| 237 | 2s 2p <sup>6</sup> 3p 3d                        | o | <sup>4</sup> F <sub>7/2</sub> | -                 | 7729551         | 7721465            | -                   |
| 238 | 2s 2p <sup>6</sup> 3p 3d                        | o | <sup>4</sup> F <sub>9/2</sub> | -                 | 7740363         | 7731661            | -                   |
| 239 | 2s 2p <sup>6</sup> 3p 3d                        | o | <sup>2</sup> D <sub>5/2</sub> | -                 | 7749958         | 7740486            | -                   |
| 240 | 2s 2p <sup>6</sup> 3p 3d                        | o | <sup>2</sup> D <sub>3/2</sub> | -                 | 7753184         | 7743954            | -                   |